

**Evaluating heat vulnerability and the impact of urban street
tree planting on radiant heat exposure: examples from
Vancouver's neighborhoods**

by

Mehdi Aminipouri

M.Sc. (Environmental Sciences), University of Southampton, 2009

B.Sc. (Statistics), University of Tabriz, 2005

Thesis Submitted in Partial Fulfillment of the
Requirements for the Degree of
Doctor of Philosophy

in the

Department of Geography

Faculty of Environment

© Mehdi Aminipouri 2019

SIMON FRASER UNIVERSITY

Summer 2019

Approval

Name: Mehdi Aminipouri

Degree: Doctor of Philosophy (Geography)

Title: Evaluating heat vulnerability and the impact of urban street tree planting on radiant heat exposure: examples from Vancouver's neighborhoods

Examining Committee:

Chair: Geoff Mann
Professor

Kirsten Zickfeld
Senior Supervisor
Associate Professor

Anders Knudby
Supervisor
Associate Professor
Department of Geography, Environment and Geomatics
University of Ottawa, Canada

Ariane Middel
Supervisor
Assistant Professor
School of Arts, Media and Engineering
Arizona State University, USA

Scott Krayenhoff
Supervisor
Assistant Professor
School of Environmental Sciences
University of Guelph, Canada

Tim Takaro
Internal Examiner
Professor, Faculty of Health Sciences

James Voogt
External Examiner
Associate Professor
Department of Geography
Western University, Canada

Date Defended/Approved: June 13, 2019

Abstract

Extensive impervious surface cover, anthropogenic heat, building structure and lack of vegetation contribute to the formation of distinct urban microclimates where higher air and surface temperature as well as lack of shade intensify outdoor heat exposure and thermal discomfort for humans. The objectives of this thesis are to explore the determinants of heat vulnerability across Vancouver's neighborhoods and assess the impact of increasing street tree cover on extreme radiant heat exposure in different neighborhoods classified into local climate zones (LCZs) under present and future climate. To achieve these goals, first, the determinants of heat vulnerability in Vancouver's neighborhoods were identified and population groups most vulnerable to extreme heat exposure were mapped by spatially superimposing multiple layers of socio-economic, environmental, and infrastructural data. Secondly, the influence of added street trees on radiant heat exposure across six different LCZs was investigated under present climate. This was done by employing the SOLar and LongWave Environmental Irradiance Geometry (SOLWEIG) model. The radiant cooling effect of increased street tree cover during the hottest day on record for Vancouver (July 29, 2009) was modeled by quantifying the spatiotemporal changes to mean radiant temperature (T_{mrt}). Results indicated a 2.1–4.2 °C reduction in spatially-averaged T_{mrt} during the hottest period of day. Lastly, this thesis sought to explore how changes in temperature and solar radiation under future climate projections would change T_{mrt} in Vancouver over the 2070-2100 period and the extent to which these changes could be mitigated by increased street tree cover. To this scope SOLWEIG was driven with downscaled climate projections using Representative Concentration Pathways (RCP) 4.5 and 8.5. Results showed that days with extreme radiant heat exposure were predicted to increase three- to five-fold under RCP 4.5 and 8.5, respectively. The addition of street trees can mitigate the increase in T_{mrt} under RCP 4.5 but is not sufficient to compensate for the T_{mrt} increase under RCP 8.5.

The results of this thesis provide valuable insights to city decision-makers and urban planners regarding effective heat mitigation and adaptation interventions and guide future research seeking to simulate the effect of heat mitigation measures under current and future climates.

Keywords: Radiant heat exposure; Micrometeorological modelling; SOLWEIG; Urban tree planting; Mean radiant temperature; Local climate zones.

Dedication

*To my dear wife, **Maedeh***

*My sons, **Amir and Ali***

With endless love and gratitude

Acknowledgements

Worship and adoration to almighty God, the most gracious, the most merciful

Utmost appreciation and heartfelt gratitude to:

- My parents for their immense support.
- Dr. Anders Knudby for his tireless guidance, inspiration and encouragement.
- Dr. Kirsten Zickfeld for her generous and unwavering support.
- PhD committee members, Dr. Scott Krayenhoff and Dr. Ariane Middel for their valuable time and feedback.
- University of Gothenburg research team, Prof. Sofia Thorsson, Dr. Fredrik Lindberg and Dr. David Rayner for their kind hospitality and tremendous technical assistance.
- Pacific Institute for Climate Solutions (PICS) and Mathematics of Information Technology and Complex Systems (MITACS) Globalink research fellowship programs for their financial support.

Table of Contents

Approval.....	ii
Abstract.....	iii
Dedication	v
Acknowledgements	vi
Table of Contents	vii
List of Tables	ix
List of Figures	x
Chapter 1. Introduction	1
1.1. Background.....	1
1.2. Objectives, Study Area, and Thesis Structure.....	3
1.2.1. Objectives	3
1.2.2. Study area.....	3
1.2.3. Thesis structure	4
1.3. References	4
Chapter 2. Using multiple disparate data sources to map heat vulnerability: Vancouver case study.....	8
2.1. Abstract.....	8
2.2. Introduction	9
2.2.1. Background	10
2.2.2. Compilation of heat vulnerability indicators	13
2.2.3. Environmental and infrastructural data	16
2.2.4. Socio-economic data	17
2.2.5. Spatial overlay and visual analysis	17
2.3. Results.....	18
2.4. Discussion	21
2.5. Conclusion	23
2.6. Acknowledgements.....	23
2.7. References	23
Chapter 3. Modelling the impact of increased street tree cover on mean radiant temperature across Vancouver’s local climate zones	31
3.1. Abstract	31
3.2. Introduction	32
3.3. Materials and methods.....	35
3.3.1. Study area.....	35
3.3.2. SOLWEIG.....	35
3.3.3. SOLWEIG evaluation.....	37

3.3.4.	Increased street tree scenario	40
3.4.	Results and discussion	41
3.4.1.	Evaluation of SOLWEIG with field measurements.....	41
3.4.2.	Spatial patterns of T_{mrt}	42
3.4.3.	Effects of increased street tree cover	44
3.5.	Conclusion	48
3.6.	Acknowledgments.....	48
3.7.	References	49
Chapter 4. Urban tree planting and outdoor thermal comfort in the face of global warming: The case of Vancouver’s local climate zones		53
4.1.	Abstract	53
4.2.	Introduction	54
4.3.	Materials and methods.....	57
4.3.1.	Study area.....	57
4.3.2.	Meteorological data	57
4.3.3.	Climate change scenarios.....	58
4.3.4.	Projected changes in meteorological variables and assessment of extreme radiant thermal exposure.....	61
4.3.5.	Simulations of T_{mrt} in SOLWEIG	61
4.4.	Results and discussion	63
4.4.1.	Projected changes in micrometeorological variables	63
4.4.2.	Spatial variations of T_{mrt} under RCP 4.5 and 8.5	68
4.4.3.	The effect of street trees on T_{mrt}	70
4.5.	Conclusion	73
4.6.	Acknowledgments.....	74
4.7.	References	74
Chapter 5. Conclusions		80
5.1.	Overall contributions.....	80
5.2.	Discussion	82
5.3.	General conclusion and future outlook.....	84
5.4.	References	84

List of Tables

Table 2-1:	Heat vulnerability indicators. Adopted from San Francisco Department of Public Health (SFDPH 2013).	14
Table 2-2:	Proposed categories of heat vulnerability indicators for which geospatial data are available for Vancouver.	17
Table 3-1:	The correlation between measured and modelled T_{mrt} ($^{\circ}\text{C}$) is shown for two time periods: all day (9:00-18:00) and hottest period of day (11:00-17:00). For each LCZ, R^2 , mean absolute error (MAE, $^{\circ}\text{C}$) and root mean square error (RMSE, $^{\circ}\text{C}$) are stated.	40
Table 3-2:	Spatial average of T_{mrt} before and after adding street trees. The data is shown for two time periods: all day from 9:00 – 18:00 and the hottest period of day from 11:00 – 17:00. ΔT_{mrt} measures the reduction in T_{mrt} due to 1% increase in street tree coverage.	45
Table 4-1:	Average number of days per year, average number of consecutive days (two or more days) per year and average number of weeks (seven consecutive days) per year with $T_{mrt} \geq 65^{\circ}\text{C}$ for observation period, RCP 4.5 and 8.5 scenarios.	70
Table 4-2:	Spatial average of T_{mrt} values before and after adding maximum feasible street trees. Results are for the hottest period of day from 11:00 – 17:00 for the hottest day in the observation period, RCP 4.5 and 8.5. Δ indicates the difference in T_{mrt} relative to the observation day under current tree cover.	71

List of Figures

- Figure 2-1: Polygons represent DAs in the top 25% most vulnerable areas for one or more indicators. Each map highlights DAs based on the number of co-existing vulnerability indicators—those in the top 25% for: (a) at least 5 out of 6 indicators; (b) 4 out of 6 indicators; (c) 3 out of 6 indicators; and (d) 2 out of 6 indicators. Map background shows spatial variations in land surface temperature..... 20
- Figure 2-2: Polygons 1, 2, and 3 indicate vulnerable DAs far from health/cooling infrastructure. (a) This map represents the 3-out-of-6 category. Polygon 1 falls outside the distance thresholds for cool shelters and the rapid transit network. (b) This map represents the 2-out-of-6 category. Polygons 2 and 3 fall outside the distance thresholds for cool shelters, drinking fountains, and the rapid transit network.22
- Figure 3-1: Aerial view and sky view of 6 LCZs in Vancouver. The study areas are: (a) LCZ 1 compact high-rise; (b) LCZ 4 open high-rise; (c) LCZ 5 open-mid-rise; (d) LCZ 6 open low-rise; (e) LCZ 6A open low-rise with dense trees; and (f) LCZ 8 large low-rise. 36
- Figure 3-2: Measuring equipment used for the validation of simulated T_{mrt} values. 38
- Figure 3-3: Existing and added street trees for the 1% increase in street tree cover scenarios, overlaid on the BDSMs at each LCZ..... 42
- Figure 3-4: Variation of T_{mrt} values for six LCZs in Vancouver. The T_{mrt} values are averaged over the period from 9:00 – 18:00 for July 29, 2009..... 44
- Figure 3-5: Variation of T_{mrt} values for 1% increase in street tree coverage in six LCZs in Vancouver. The T_{mrt} values are averaged over the period from 9:00 – 18:00 for July 29, 2009..... 46
- Figure 3-6: Change (ΔT_{mrt}) in the spatial distribution of T_{mrt} values before and after street tree inclusion scenarios in the simulation domain. The T_{mrt} values are averaged over the period from 9:00 – 18:00 for July 29, 2009 in six LCZs in Vancouver. 47
- Figure 4-1: The location of selected LCZs and climate tower station in Vancouver, British Columbia, Canada..... 58
- Figure 4-2: Aerial view and sky view of selected LCZs in Vancouver. The study areas are: LCZ 1 compact high-rise; LCZ 4 open high-rise; LCZ 5 open-mid-rise; LCZ 6 open low-rise; LCZ 6A open low-rise with dense trees; and LCZ 8 large low-rise. 60
- Figure 4-3: (a) Observed monthly-averaged daily maximum and minimum T_a across the annual cycle; (b) difference between observed and future RCP 4.5 and 8.5 scenarios in monthly-averaged daily maximum T_a across the annual cycle; (c) difference between observed and future RCP 4.5 and 8.5 scenarios in monthly-averaged daily minimum T_a across the annual cycle. Observation record is from 2008-2017 and climate scenarios are from 2070-2100..... 65
- Figure 4-4: (a) observed monthly-averaged daily global shortwave radiation; (b) difference between RCP 4.5 and 8.5 scenarios and observation period in monthly-averaged daily global shortwave radiation. Observation record is from 2008-20171 and climate scenarios are from 2070-2100..... 67

Figure 4-5: (a) Observed monthly-averaged daily maximum and minimum T_{mrt} across the annual cycle; (b) difference between observed and future RCP 4.5 and 8.5 scenarios in monthly-averaged daily maximum T_{mrt} across the annual cycle; (c) difference between observed and future RCP 4.5 and 8.5 scenarios in monthly-averaged daily minimum T_{mrt} across the annual cycle. Observation record is from 2008-2017 and climate scenarios are from 2070-2100..... 69

Figure 4-6: The spatial variation of T_{mrt} in present climate (left column) and the combined effect of climate change and increased street tree cover for RCP 4.5 and 8.5 scenarios (middle and right column). Δ RCP 4.5 and Δ RCP 8.5 present change in T_{mrt} values relative to the observation day after the inclusion of maximum feasible street tree in the simulation domain. The T_{mrt} values are averaged over the period from 11:00 – 17:00. For illustration purposes, the comparison is only shown for LCZ 4 and 5..... 72

Chapter 1. Introduction

1.1. Background

Urban areas create distinct environments that are different from their rural surroundings in terms of impervious surface and vegetation cover, building and street geometry, wind exposure, as well as anthropogenic heat generation. Impervious surfaces such as asphalt and concrete absorb and release large amounts of heat, and due to their impermeability to water they significantly reduce the potential for evaporative cooling. These urban characteristics alter micrometeorological conditions in the urban canopy layer (ground to roof level) such that cities are relatively warmer than their immediate rural surroundings, a phenomenon also known as the urban heat island (UHI) effect (Arnfield, 2003; Oke, 1982). The UHI intensity varies diurnally and seasonally (Doick et al. 2014). In most midlatitude temperate climate cities, nocturnal UHI effect is greater than daytime UHI effect (Oke 1981). In Vancouver for example, a nocturnal UHI (i.e. difference in near-surface air temperature between urban and rural areas) as high as 9°C was observed by Runnalls and Oke (2000). The UHI effect is significant because with more intense, frequent and long-lasting heatwaves expected to occur under global warming (IPCC 2014), the excess warmth in cities is projected to have significant impact on heat vulnerability, heat exposure, human health (Argüeso et al., 2015; Kenny et al., 2010; Perkins et al. 2012; Stewart and Oke, 2012; Taleghani et al., 2016).

Extreme heat conditions are linked to increased mortality from heat stroke, heat exhaustion, cardiovascular and respiratory diseases (Luber and McGeehin 2008; Petkova et al. 2014). The 2003 lethal heatwave in France and the 1995 heatwave in Chicago, USA resulted in 15,000 and 700 excess deaths, respectively. Extreme heat conditions are not only associated with excess mortality, but also heat-related morbidity. In the literature, heat-related morbidity has been assessed using various indicators, including for example excess number of hospital admissions and heat-related medical dispatches during extreme heat events. (Fouillet et al. 2006; Semenza et al. 1996). Compared to suburban and rural residents, the health condition of urban dwellers is thought to be more affected by extreme heat, since they live in settings where air and surface temperatures are often higher than their suburban and rural surroundings.

These urban settings exacerbate the risk of heat-related mortality and morbidity particularly among elderly residents, infants, ethnic minorities, and those with low socioeconomic status (Kovats and Hajat 2008). Studies of heat vulnerability and extreme radiant heat exposure have attracted considerable attention worldwide, with most research evaluating the effect of present-day climate over large regions (Inostroza et al., 2016; Wolf et al., 2014). The extent to which projected changes in climate will affect radiant heat exposure across single urban neighborhoods has never been assessed for Vancouver. While vulnerability to heat and extreme radiant heat exposure is less severe in mid- and high-latitude cities, such as Vancouver, than in low-latitudes (Thorsson et al., 2017), it can lead to severe heat stress due to poor acclimatization of northern, and especially coastal populations to extreme heat (Rocklöv and Forsberg, 2008; Watkins et al., 2007). However, not all neighborhoods and populations are impacted equally. The health effects of extreme heat events and vulnerability to heat depend on risk perceptions among different vulnerable populations (Howe et al. 2019), population characteristics (e.g. socioeconomic status, age, unemployment rate, etc.) and the built and natural environments (Vescovi et al. 2005; Rinner et al. 2010). Regarding the built and natural environment, elements linked to e.g. building structure, and vegetation cover influence heat variability and exposure across different neighborhoods (Rasanen et al. 2019). Understanding the spatial overlap of these built and natural environment elements with population characteristics of heat vulnerability is of great importance to policymakers and health professionals (He et al. 2019; Spangler et al. 2019). It is therefore crucial to explore how heat exposure and vulnerability differ among different neighborhoods under current and future climate. This examination of heat vulnerability and exposure offers the potential to properly plan heat mitigation interventions.

For the purpose of this thesis, heat vulnerability is defined as a function of three interactive components: exposure (e.g. extreme heat), sensitivity (e.g. population characteristics) and coping capacity (e.g. access to cooling and health infrastructure) (Wilhelmi and Hayden 2010).

Hence, the goal of this thesis is to explore the determinants of heat vulnerability and assess the impact of one particular heat mitigation measure (i.e. increasing street tree cover) on extreme radiant heat and outdoor thermal exposure in the coastal mid-latitude city of Vancouver.

1.2. Objectives, Study Area, and Thesis Structure

1.2.1. Objectives

The overall aim of this thesis is twofold:

- a) To identify determinants of heat vulnerability and to increase understanding of how vulnerability to heat varies across Vancouver's neighborhoods. The goal here is to provide an initial assessment of heat-vulnerable neighborhoods in Vancouver. Heat mitigation measures can be further investigated in those vulnerable neighborhoods using the local climate zones (LCZs) approach proposed in the next objective.
- b) To investigate how the addition of urban street trees influences radiant heat exposure across Vancouver's LCZs, under present and future climates.

Specific objectives are to:

- Integrate multiple disparate data to spatially visualize co-occurrence of heat exposure, heat sensitivity and lack of heat coping resources to assess vulnerability in Vancouver's neighborhoods (Chapter 2).
- Assess the spatiotemporal variation of T_{mrt} and its daytime reductions resulting from increased street tree cover within street sections of representative LCZs in Vancouver (Chapter 3)
- Investigate the radiant cooling potential of increased street tree cover under two projected climate scenarios for selected LCZs in Vancouver (Chapter 4).

1.2.2. Study area

The field measurements and the simulations in this thesis were conducted in Vancouver, British Columbia, Canada (Figure 4.1). Vancouver lies on a peninsula in the southwestern corner of the province of British Columbia (49.2°N, 123.1°W), has a western maritime climate with annual mean air temperature of 14°C, mild winters and semi-dry summer months. The city is located on the British Columbia's west coast and lies between Burrard Inlet to the north and

Fraser River valley and its floodplains to the south. Combined with the range of urban densities found in the area, this environmental context produces substantial differences in thermal environment between different parts of the city (Ho et al., 2016). Living in a mild oceanic climate, Vancouverites are generally less adapted to probable future heat waves which makes this city a suitable case for assessing the differential influence of extreme radiant temperature and heat events across neighbourhoods.

1.2.3. Thesis structure

The rest of this thesis consists of three peer-reviewed publications in the form of stand-alone chapters (Chapter 2, 3 and 4) that each address one of the specific objectives outlined earlier, as well as a concluding chapter (Chapter 5). The first paper (Chapter 2), which was published in the *Canadian Geographer*, reviews determinants of heat vulnerability from around the world and investigates the relevance of those determinants to Vancouver. This paper serves as a baseline for characterizing heat vulnerability across Vancouver's neighborhoods. While heat-vulnerable neighborhoods are identified in this paper, further investigation on how radiant heat exposure can be reduced in those neighborhoods was necessary. Thus, in the second paper (Chapter 3), which was published in *Urban Forestry and Urban Greening*, the effect of increased street tree cover on mean radiant temperature across different neighborhoods classified into LCZs was simulated using the SOLar and LongWave Environmental Irradiance Geometry (SOLWEIG) model. However, with climate change, requirements for heat mitigation strategies at street-level to moderate pedestrian thermal exposure are changing. Therefore, in the third paper (Chapter 4), in review at *Building and Environment* in February 2019, the influence of adding the maximum feasible number of street trees on radiant heat exposure was modelled for current climate and projected changes under two downscaled climate scenarios. Chapter 5 concludes the thesis by highlighting the contribution of each paper and outlining the limitations of this work.

1.3. References

Argüeso, D., Evans, J.P., Pitman, A.J., Di Luca, A., 2015. "Effects of city expansion on heat stress under climate change conditions." *PLoS One*. 10, 1–19.

- Arnfield, A.J., 2003. "Two decades of urban climate research: a review of turbulence, exchanges of energy and water, and the urban heat island." *International Journal of Climatology*. 23, 1–26.
- Doick, K.J., Peace, A., Hutchings, T.R., 2014. "The role of one large greenspace in mitigating London's urban heat island."
- Fouillet, A., G. Rey, F. Laurent, G. Pavillon, S. Bellec, C. Guihenneuc-Jouyau, J. Clavel, E. Jougl, and D. Hémon. 2006. "Excess mortality related to the August 2003 heat wave in France." *International Archives of Occupational and Environmental Health*. 80 (1): 16–24.
- He, C., Ma, L., Zhou, L., Kan, H.D., Zhang, Y., Ma, W.C., Chen, B., 2019. "Exploring the mechanisms of heat wave vulnerability at the urban scale based on the application of big data and artificial societies." *Environment International*. 127: 573-583.
- Ho, H.C., Knudby, A., Xu, Y., Hodul, M., Aminipouri, M., 2016. "A comparison of urban heat islands mapped using skin temperature, air temperature, and apparent temperature (Humidex), for the greater Vancouver area." *Science of the Total Environment*. 544, 929–38.
- Howe, P.D., Marlon, J.R., Wang, X., Leiserowitz, A., 2019. "Public perceptions of the health risks of extreme heat across US states, counties, and neighborhoods." *Proceedings of the National Academy of Sciences of the United States of America*. 116 (14): 6743-6748.
- Inostroza, L., Palme, M., de la Barrera, F., 2016. "A heat vulnerability index: Spatial patterns of exposure, sensitivity and adaptive capacity for Santiago de Chile." *PLoS One*. 11, 1–26.
- IPCC (Intergovernmental Panel on Climate Change). 2014. Climate Change 2014: Synthesis Report. Contribution of Working Groups I, II and III to the Fifth Assessment Report of the Intergovernmental Panel on Climate Change. Geneva, Switzerland: IPCC.
- Kenny, G.P., Yardley, J., Brown, C., Sigal, R.J., Jay, O., 2010. "Heat stress in older individuals and patients with common chronic diseases." *Canadian Medical Association Journal*. 182, 1053–1060.
- Konarska, J., Lindberg, F., Larsson, A., Thorsson, S., Holmer, B., 2014. "Transmissivity of solar radiation through crowns of single urban trees: Application for outdoor thermal comfort

- modelling." *Theoretical Applied Climatology*. 117, 363–376.
- Kovats, R.S., Hajat, S., 2008. "Heat stress and public health: a critical review." *Annual Reviews of Public Health*. 29, 41-55.
- Luber, G., McGeehin, M., 2008. "Climate change and extreme heat events." *American Journal of Preventive Medicine*. 35 (5): 429-435.
- Oke, T.R., 1981. "Canyon geometry and the nocturnal urban heat island: comparison of scale model and field observations." *Journal of Climatology*. 1: 237-254.
- Oke, T.R., 1982. "The energetic basis of the urban heat island." *Quarterly Journal of the Royal Meteorological Society*. 108, 1–24.
- Perkins, S.E., Alexander, L.V., Nairn, R.J., 2012. "Increasing frequency, intensity and duration of observed global heatwaves and warm spells." *Geophysical Research Letters*. 39 (20): L20714.
- Petkova, E.P., Morita, H., Kinney, P.L., 2014. "Health impacts of heat in a changing climate: how can emerging science inform urban adaptation planning?." *Current Epidemiology Reports*. 1 (2): 67-74.
- Rasanen, A., Heikkinen, K., Piila, N., Juhola, S., 2019. "Zoning and weighting in urban heat island vulnerability and risk mapping in Helsinki, Finland." *Regional Environmental Change*. 19 (5): 1481-1493.
- Rinner, C., Patychuk, D., Bassil, K., Nasr, S., Gower, S., Campbell, M., 2010. "The role of maps in neighborhood-level heat vulnerability assessment for the city of Toronto." *Cartography and Geographic Information Science*. 37, 31–44.
- Rocklöv, J., Forsberg, B., 2008. "The effect of temperature on mortality in Stockholm 1998—2003: A study of lag structures and heatwave effects." *Scandinavian Journal of Public Health*. 36, 516–523.
- Runnalls, K.E., Oke, T., 2000. "Dynamics and controls of the near-surface heat island of Vancouver, British Columbia." *Physical Geography*. 21 (4): 283-304.

- Semenza, J. C., C. H. Rubin, K. H. Falter, J. C. Selanikio, D. Flanders, H. L. Howe, and J. L. Wilhelm. 1996. "Heat-related deaths during the July 1995 heat wave in Chicago." *New England Journal of Medicine*. 335 (2): 84–90.
- Spangler, K.R., Manjourides, J., Lynch, A.H., Wellenius, G.A., 2019. "Characterizing spatial variability of climate-relevant hazards and vulnerabilities in the New England region of the US." *GeoHealth*. 3 (4): 104-120.
- Stewart, I.D., Oke, T.R., 2012. "Local Climate Zones for Urban Temperature Studies." *Bulletin of the American Meteorological Society*. 93, 1879–1900.
- Taleghani, M., Sailor, D., Ban-Weiss, G.A., 2016. "Micrometeorological simulations to predict the impacts of heat mitigation strategies on pedestrian thermal comfort in a Los Angeles neighborhood." *Environmental Research Letter*. 11, 24003.
- Thorsson, S., Rayner, D., Lindberg, F., Monteiro, A., Katschner, L., Lau, K.K.-L., Campe, S., Katschner, A., Konarska, J., Onomura, S., Velho, S., Holmer, B., 2017. "Present and projected future mean radiant temperature for three European cities." *International Journal of Biometeorology*. 61, 1531–1543.
- Vescovi, L., Rebetz, M., Rong, F., 2005. "Assessing public health risk due to extremely high temperature events: Climate and social parameters." *Climate Research*. 30, 71–78.
- Watkins, R., Palmer, J., Kolokotroni, M., 2007. "Increased temperature and intensification of the urban heat island: Implications for human comfort and urban design." *Built Environment*. 33, 85–96.
- Wilhelmi, O., Hayden, M.H., 2010. "Connecting people and place: a new framework for reducing urban vulnerability to extreme heat." *Environmental Research Letters*. 5 (1). 7p.
- Wisner, B. Blaikie, P., Cannon, T., Davis, I., 2003. "At risk: natural hazards, people's vulnerability and disasters." *Routledge*. 471p.
- Wolf, T., McGregor, G., Analitis, A., 2014. "Performance assessment of a heat wave vulnerability index for Greater London, United Kingdom." *Weather, Climate and Society*. 6, 32–46.

Chapter 2. Using multiple disparate data sources to map heat vulnerability: Vancouver case study

This chapter has been published in the Canadian Geographer journal.

Citation details: Aminipouri, M., Knudby, A., and Ho, H.C., 2016. "Using multiple disparate data sources to map heat vulnerability: Vancouver case study." Canadian Geographer 60, 356-368.

Contribution statement: First author designed the research, performed the analysis and wrote the manuscript. Co-authors assisted in framing the research idea, provided feedback on the interpretation of results and edited the manuscript.

2.1. Abstract

Extreme heat events have caused excess mortality in Canadian cities. In order to map the population groups most vulnerable to extreme heat in Vancouver, we overlaid multiple layers of socio-economic, environmental, and infrastructural data. By superimposing multiple disparate data layers, we were able to detect and visualize socio-economically deprived dissemination areas with high vulnerability to extreme heat events. The three dissemination areas found to be most vulnerable to heat varied from the rest of the sample in terms of environmental and infrastructural variables. These three vulnerable dissemination areas also have relatively low vegetation cover as well as relatively hot surface temperatures. As such, they are socioeconomically vulnerable, far from cooling and health infrastructure, and have an environment that elevates heat exposure. Our results are a preliminary step toward the development of tools that can help health authorities, city officials, and policymakers better understand who is at risk during extreme heat events, where they reside, what factors drive the risk, and ultimately what can be done to mitigate it.

Keywords: heat vulnerability, extreme heat events, Vancouver

2.2. Introduction

Extreme heat is a significant public health concern. The 2003 extreme heat event in Europe that resulted in 70,000 deaths and the 2010 heatwave in Russia that caused an estimated 55,000 deaths (Grize et al. 2005; Canouï-Poitrine et al. 2006; Fouillet et al. 2006; Barriopedro et al. 2011; Keller 2013) demonstrate the severe health impacts that such events can produce. With a changing climate, the frequency, duration, and intensity of extreme heatwaves are predicted to increase (IPCC 2014), leading to the intensification of health risks worldwide, including in Canada. To date, six extreme heat events have been reported in Canada over the period 1900–2009, resulting in just over 1,300 deaths (Public Safety Canada 2013; Health Canada 2011a). In Vancouver alone, an excess mortality of 122 people has been estimated for the event that occurred in the summer of 2009 (City of Vancouver 2012; Kosatsky et al. 2012).

The scientific literature exploring personal and social characteristics that increase or decrease heat vulnerability is extensive. While results vary between locations and events, typical high-risk groups include seniors, young children, people with chronic illnesses, and socially disadvantaged individuals (Health Canada 2011a, 2011b; Depietri et al. 2013; Harlan et al. 2013; Loughnan et al. 2013; Rinner et al. 2013; Loughnan et al. 2014; Rosenthal et al. 2014; Saha et al. 2014; Schuster et al. 2014). Compound effects may exist among populations who fall into multiple vulnerable categories (e.g. a low income senior), especially where such populations also suffer from environmental conditions (e.g. low vegetation cover) that increase heat exposure and/or infrastructure-related risk factors, such as poor access to cool shelters, water fountains, and health care (Buscail et al. 2012; Dugord et al. 2014). Thus, depending on the socioeconomic status and the built and natural environment characteristics, vulnerability to heat varies among different populations and spatially across neighborhoods.

Assessing and mapping such multi-faceted heat vulnerability requires the full involvement of organizations that have an existing infrastructure for generating and sharing the relevant data, which can then be integrated in a geographic information system (GIS) (IOM 2009; Citro et al. 2009). Such data have included race and ethnicity and socio-economic indicators such as median income, unemployment rate, and proportion of the population with limited official language proficiency. However, an integrated index of heat vulnerability

combining several environmental, infrastructural, and socio-economic measures has yet to be created. Spatially overlaying these disparate data can help in the location and examination of the population groups most vulnerable to heat (Reid et al. 2009; Buscail et al. 2012). For example, mapping low-income seniors who live alone in neighbourhoods with little vegetation cover and poor access to cool shelters could reveal spatial hotspots of heat vulnerability that could subsequently be addressed through public health intervention and heat mitigation measures (e.g., green roofs, reflective roofs, humidification, and increased vegetation cover) (Rizwan et al. 2008; Harlan et al. 2013).

The main goal of this work is to integrate multiple disparate data sources to spatially visualize co-occurrence of heat exposure, heat sensitivity and lack of heat coping resources in Vancouver's neighborhoods. To achieve this, indicators expected to influence heat vulnerability in Vancouver were identified; data sources that describe their spatial distribution throughout the city were explored and compiled; and a spatial overlay analysis was used to visualize areas within the city that contain multiple risk factors for heat.

2.2.1. Background

The scientific literature exploring physical and social factors related to heat vulnerability is extensive, but most studies have focused on the extreme heat event in Europe in 2003 or previous events in the United States (US). Results vary substantially by region, likely as a result of climatic, infrastructural, and societal differences, so vulnerability factors found to be important elsewhere may not be applicable to Vancouver or other urban areas in Canada. Examples of European and US studies include those by Chestnut et al. (1998), Naughton et al. (2002), Robine et al. (2008), Anderson and Bell (2009), García-Herrera et al. (2010), and Alcoforado et al. (2015), and vulnerability indicators for the Canadian context have been summarized by Kosatsky et al. (2005), Pengelly et al. (2007), Rinner et al. (2013), and Belanger et al. (2015). The literature review presented in the next two sections focuses on heat vulnerability indicators from cities with a climate similar to Vancouver's (i.e., within the Pacific Northwest (PNW), including Vancouver, Seattle, Portland, and San Francisco), with lesser consideration of evidence from other climates. The following sub-sections provide an overview of the

relationship between extreme heat and human health, and past extreme heat events in the PNW region.

2.2.1.1. Extreme heat and human health

The relationships between extreme heat, health risks, mortality, and morbidity have been studied extensively (Chestnut et al. 1998; Braga et al. 2001; Curriero et al. 2002; Medina-Ramón et al. 2006; Mastrangelo et al. 2007). Long exposure to extreme heat can severely affect a person's physiological comfort, resulting in heat stress and, in extreme cases, death (Luber et al. 2006; Reid et al. 2009). Not all populations are equally vulnerable to the risks associated with extreme heat. Variations in the distributions of neighbourhoods' socio-economic status, environmental exposures, and infrastructural factors affect heat vulnerability. Several studies have listed a range of factors that influence vulnerability to extreme heat events on an individual and neighbourhood scale, including but not limited to: local climate, age, income, housing, health status, access to cool places, and a social network (Harlan et al. 2013; Coates et al. 2014; Gronlund et al. 2014; Belanger et al. 2015; Hondula et al. 2015; Onozuka and Hagihara 2015). However, studies of health impacts of extreme heat events should consider not only who is vulnerable to heat, but also where the vulnerable populations reside (Smoyer 1998). Vulnerability variables at these levels include environmental exposure factors (e.g., temperature, air quality, tree density, proximity to parks/green space, living on top floor), and infrastructure conditions (e.g., building age, mobility/access to transportation, air conditioning).

2.2.1.2. Extreme heat in the PNW region

The PNW, which includes southwestern British Columbia (BC) and the western reaches of Washington and Oregon in the US, typically experiences a mild summer climate with few instances of extreme heat events. The 2009 event set all-time high temperature records throughout western Washington and southern BC (Bumbaco et al. 2013). This specific event had significant health impacts because the PNW region is not historically prone to extreme heat, and residents are likely to experience greater negative impacts and increased mortality due to the relative rarity of occurrence (Meehl and Tebaldi 2004).

The extreme heat event in summer 2009 in Vancouver alone caused an estimated 122 excess deaths and many emergency room visits (City of Vancouver 2012; Kosatsky et al. 2012). During the end of July and beginning of August 2009, the maximum and minimum temperatures at Vancouver International Airport were 30.9°C (19.6°C) on July 28, 34.0°C (20.2°C) on July 29, and 34.4°C (22.4°C) on July 30, all under clear skies with an average relative humidity of 57%. Within days of the onset of the hot weather event, BC's rapid mortality surveillance system indicated that deaths among residents of greater Vancouver had increased by around 40% for the period through August 2 (Kosatsky et al. 2012). Residents of Vancouver are generally not acclimatized to extreme heat events during the summer months, and as a result have a relatively low threshold and quickly suffer heat-related consequences (Henderson et al. 2013). Vulnerable segments of the population, including seniors, infants, persons with chronic illness, and socio-economically disadvantaged individuals, are at relatively higher risk (City of Vancouver 2012; Kosatsky et al. 2012).

From 1980 to 2010, mortality rates associated with extreme heat in King County, Washington were quantified in a study conducted by Isaksen (2014). The results demonstrate that heat, expressed as a humidex (Basu 2009; Zhang et al. 2014), is associated with increased non-trauma mortality and hospital admissions on extreme hot days, and that risk increases with heat intensity, especially among older individuals. Isaksen (2014) found that on hot days—those above the 99th percentile—the all-ages relative risk for mortality was roughly 10% higher when compared to that on a “non-hot” day. This risk was found to increase 2.12% for every degree increase in the humidex above 36.0°C. Similarly, the all-ages relative risk of hospitalization on a hot day was found to be 2% greater when compared to that on a non-hot day—reflecting an increase of 1.59% for each degree increase in the humidex above 37.4°C (Isaksen 2014). While those in the 65+ age group were found to be at greater risk of poor health outcomes on an extreme hot day, younger age groups were also found to be at risk for specific causes of death and hospitalization (Isaksen 2014).

Given that direct quantitative assessment of vulnerability is often difficult (Cutter et al. 2010), a comparative approach to assessment can be employed by considering variables and indicators that act as proxies for vulnerability to heat. This indicator approach to vulnerability measurement, however, has been criticized for its subjectivity with regard to both the selection and weighting of variables, its dependence on data availability, and its issues with spatial scales

and validation of the results (Luers et al. 2003; Malone and Brenkert 2008). Nonetheless, these indicators are valuable for planners and decision makers as they provide accessible metrics for vulnerability that support priority setting, mapping, and progress measurement for public health interventions (Cutter et al. 2008).

Depending on the area of interest and availability of data, a variety of health conditions such as diabetes and respiratory illnesses among residents have also been considered as indicators for heat vulnerability (Reid et al. 2009; Kosatsky et al. 2012). However, a consistently measured local dataset that contains locational data (i.e., geographical coordinates) does not currently exist for the majority of these pre-existing individual health factors, thus making it impossible to identify and map the vulnerable population in this sense. The only heat-mortality relationship study from Vancouver, conducted by Kosatsky et al. (2012), examined patterns of mortality during the extreme heat event in summer 2009, considering age, sex, location of death (home vs. other), population density, elderly people living alone, and poverty as vulnerability factors. Kosatsky et al. (2012) found that the 65–74 years age group was at significantly higher risk than the reference group (≥ 85 years old), while those under age 65 and those aged 75–84 years were not at significantly higher risk. This study also found that men were at marginally higher risk than women, and people in hospitals and care residences were at significantly lower risk than people living at home. People living in areas with high population density, areas where more than 40% of people aged 65 years and older lived alone, and areas where more than 20% of people lived in poverty, were also at higher risk (Kosatsky et al. 2012). Although not all these findings were statistically significant, parallel findings in several studies from Europe and the US support their validity. Analyses of extreme heat events in Canada, the US, and Europe reveal indicators that modify the relationship between heat, morbidity, and mortality. Table 2.1 outlines many of the variables that impact heat vulnerability, including socio-economic status, environmental exposure, and infrastructural factors, and briefly describes their effects on health during an extreme heat event. Data and methodology

2.2.2. Compilation of heat vulnerability indicators

In compiling heat vulnerability indicators relevant to the PNW region, evidence from Vancouver (Kosatsky et al. 2012), other Canadian cities (Pengelly et al. 2007; Health Canada

2011a, 2011b; Price et al. 2013; Rinner et al. 2013), San Francisco (SFDPH 2013), and Washington state (Jackson et al. 2010; Bumbaco et al. 2013; Isaksen 2014) have been taken into consideration (see Table 2.2). The highest-resolution, smallest-area data available in Vancouver were at the level of the Census Dissemination Area (DA), a small area composed of one or more neighbouring dissemination blocks, with a population of 400 to 700 persons (Statistics Canada 2015).

Table 2-1: Heat vulnerability indicators. From San Francisco Department of Public Health (SFDPH 2013).

Factors	Heat vulnerability	Data	Effects of indicator on human health during extreme heat events
	indicator		
Demographic and Socio-economic Factors	Age: infants and children	Proportion of population aged 0-4	This particular population group is more vulnerable to heat for the following reasons: reduced ability to thermo-regulate, increased risk for dehydration, and reduced ability to communicate discomfort to caregivers (Luber et al. 2006).
	Age: elderly	Proportion of population aged ≥65	Higher mortality risk for populations above the age of 65 (Knowlton et al. 2009; Kosatsky et al. 2012), as well as higher hospital admission rate for respiratory and other heat-related diseases (Kilbourne et al. 1982).
	Race/Ethnicity	Proportion of non-white population	Data has shown that race/ethnicity is a common heat vulnerability factor (Klinenberg 1999; O’Neill et al. 2003; Medina-Ramon et al. 2006).
	Level of Education	Proportion of population 25+ without a high school degree	Socio-economic status—including percentage of persons without a high school education, low median household incomes, and percentage of those living in poverty—have been shown to be highly associated with increased heat stress (Harlan et al. 2006), mortality (Curriero et al. 2002), and increased risk of heat-related morbidity (Jones et al. 1982).
	Income	Average household income	
	Poverty	Proportion of population below poverty line	
	Language Barrier	Proportion of population defined as linguistically isolated	Vulnerability may increase in the absence of linguistically suitable heat-warning systems and the inability for health care providers to communicate with non-English speakers (Sheridan 2007).
	Nursing Home	Proportion of population living in a nursing home	Elderly living in senior care facilities have been found to be at increased risk for mortality (Klinenberg 1999; Fouillet et al. 2006).
	Social Isolation	Proportion of population living alone	Persons living alone, especially those above the age of 65, are more vulnerable to heat (Klinenberg 1999; Harlan et al. 2006).

Factors	Heat vulnerability	Data	Effects of indicator on human health during
	indicator		extreme heat events
Environmental Exposure Factors	Population Density	Population density (persons/square mile)	Densely populated areas have been associated with higher heat stress levels (Harlan et al. 2006).
	Surface/air temperature & Humidex	Mean/minimum/maximum daily temperature	Remote sensing techniques have been used frequently to study urban microclimates and predict surface and air temperatures as well as humidex (Ho et al. 2014).
	Air Quality	Maximum PM _{2.5} concentration (µg/m ³)	The concentration of air pollutants may change due to weather patterns at different spatial scales. The concentration of air pollutants such as ozone, particulates, and nitrogen dioxide increase during extreme heat events and can ultimately exacerbate air pollution-related mortality (Knowlton et al. 2004; Papanastasiou et al. 2015).
	Park accessibility	Proportion of population with limited park accessibility (more than 200 meters of a park)	Air temperature is reduced around 1.8°F for every 100 m ² of vegetation added to a park (Dimoudi and Nikolopoulou 2003).
	Tree Density	Number of trees per square mile	The presence of greenery in an urban neighborhood will help mitigate the adverse health effects of extreme heat events, leading to decreases in air temperature (Dimoudi and Nikolopoulou 2003; Vandentorren et al. 2006).
	Proximity to water bodies and drinkable water fountains	Distance to major water bodies and also relative extent of the water bodies	Irrigated land and water bodies can cool surroundings due to increased evaporation and thus alleviate human discomfort during heat events (Buscail et al. 2012; Dugord et al. 2014). Drinking fountains may provide a point of rehydration outside the home.
Infrastructure Conditions	Building Age	Average age of building	Lack of thermal insulation in old buildings has been recognized as a main risk factor during past extreme heat events (Vandentorren et al. 2006).
	Air Condition Prevalence	Proportion of population without central air conditioning	Access to air conditioning has been documented frequently as a factor determining heat-related morbidity and mortality (Semenza et al. 1996; Curriero et al. 2002; Bouchama et al. 2007; Reid et al. 2009).
	Transportation accessibility	Proportion of population that doesn't live within 0.5 miles of a transit station	Access to transportation (either car, bus, or train) can reduce the risk of heat-related mortality (Semenza et al. 1996).
	Housing Conditions: living on the top floor	Proportion of population living in the building's top floor	Living on the top floor in a multi-story building has been found to increase the risk of heatstroke and mortality during extreme heat events (Kilbourne et al. 1982; Vandentorren et al. 2006).

2.2.3. Environmental and infrastructural data

Geospatial data describing the spatial distribution of all the infrastructural and some of the environmental vulnerability indicators from Table 2.2 were downloaded from the City of Vancouver's Open Data Catalogue (City of Vancouver 2015). These include the locations of parks, water bodies, cool shelters (including community centres, homeless shelters, and libraries), public transportation routes and stations, hospitals, and drinking fountains.

Maximum air temperature, land surface temperature, and humidex for typical hot summer days, quantified relative to Vancouver International Airport, were obtained from Ho et al. (2014). All temperature maps have been derived as a 4-day average (13 August 2002; 17 July 2004; 23 July 2006; 12 July 2008) using cloud-free Landsat TM/ETM+ satellite images taken during hot summer days (maximum air temperature higher than 25°C at YVR International Airport). These temperature map products are all in raster format with 60-metre spatial resolution. Little variation existed between the three different temperature maps, and only the land surface temperature map was used for visualization purposes.

The land surface temperature data were resampled to the DAs to align with the socio-economic data. While a higher spatial resolution could have been obtained by resampling the census data to the 60-metre resolution of the temperature data layers (Ho et al. 2015), use of the resulting intra-DA temperature variability in combination with the census data would implicitly assume that the census data of a DA are equally valid for all raster cells in that DA. This assumption leads to the ecological fallacy; for example, in a DA with a vulnerable population, a hot parking lot would be identified as having an elevated heat risk, despite nobody residing in that precise location. We therefore chose to retain the DAs as the spatial unit of analysis.

Vegetation cover was quantified from the Landsat TM/ETM+ data using the Normalized Difference Vegetation Index (NDVI), which quantifies the amount and health of vegetation (Imhoff et al. 2010; Anniballe et al. 2014). NDVI values range from -1.0 (deep water with no vegetation) to 1.0 (healthy vegetation). The vegetation cover map was similarly resampled to the DAs to match the spatial scale of the socio-economic data.

2.2.4. Socio-economic data

The socio-economic data were obtained from the 2006 Canadian Census (Statistics Canada 2006). The data are freely available in tabular format and are spatially aggregated by DA. The following data were obtained: persons aged 65 years and over living alone; low-income persons 15 years and older (i.e., less than \$30,487 after-tax); total population speaking a non-official Canadian language; unemployment rate; infants aged 0–4 years; and persons aged 65–74 years.

Table 2-2: Proposed categories of heat vulnerability indicators for which geospatial data are available for Vancouver.

Socio-economic	Environmental	Infrastructural
<ul style="list-style-type: none"> • Age • Unemployment rate • Social isolation (elderly living alone) • Population density • % of population speaking a non-official Canadian language • Income 	<ul style="list-style-type: none"> • Land surface temperature • Air temperature • Humidex • Vegetation cover • Proximity to parks • Proximity to water bodies 	<ul style="list-style-type: none"> • Proximity to cool shelters (community centres, homeless shelters, libraries) • Proximity to public transportation • Proximity to hospitals • Proximity to drinking fountains

2.2.5. Spatial overlay and visual analysis

The DAs in Vancouver were ranked according to each of the six socioeconomic vulnerability indicators, and for each indicator the top 25% most vulnerable areas were identified. We then examined the presence of different vulnerability factors in each DA. DAs were categorized according to the prevalence of their vulnerability factors, namely DAs in the top 25% for: (1) at least 5 out of 6 indicators; (2) 4 out of 6 indicators; (3) 3 out of 6 indicators; and (4) 2 out of 6 indicators. The 25% threshold was chosen subjectively in an exploratory fashion to arrive at an easily interpretable number for designating high vulnerability areas. The 25% cut-off is easy for city officials to replicate without using complex statistical procedures and

thus it facilitates decision making and directing efforts toward areas most in need of heat mitigation plans.

Infrastructural factors such as proximity to cool shelters (i.e., libraries, community centres, and homeless shelters), drinking fountains, rapid transit, and hospitals, as well as the land surface temperature, were then spatially overlaid to produce maps that combine information on heat exposure, heat vulnerability, and related infrastructure. The presence of socially disadvantaged groups, such as elderly living alone or low-income families with infants, may spatially coincide with very hot neighbourhoods leading to a higher heat-related health risk. Where high vulnerability areas are also hot and/or not in close proximity to cool shelters, drinking fountains, rapid transit network, and hospitals, the combination of high vulnerability, exposure, and lack of cooling/health infrastructure makes such areas of particular interest for potential public health intervention or heat mitigation measures. For the purposes of this study, poor accessibility to city amenities that are useful in the presence of extreme heat events, including cool shelters, drinking fountains, rapid transit network, and hospitals, has been defined as follows: being one kilometre away from cool shelters, hospitals, and rapid transit network and being 500 metres from drinking fountains. We delineated the areas of influence around the cooling/health infrastructure using the Euclidean Buffer tool in ArcGIS.

2.3. Results

By superimposing multiple disparate data layers, we were able to detect and visualize socio-economically deprived DAs with high vulnerability to extreme heat events. Four DAs are in the top 25% of at least 5 out of the 6 vulnerability factors (Figure 2.1a), a number that increases to 10 DAs for the 4-out-of-6 indicators category (Figure 2.1b); 29 DAs for the 3-out-of-6 category (Figure 2.1c); and 62 DAs for the 2-out-of-6 category (Figure 2.1d). No DA was in the top 25% of all six vulnerability factors.

Almost all detected DAs are located within relatively hot areas of the city, indicating a low density of green space and high percentage of impervious surfaces, a combination considered to be an immediate heat-related health risk factor (Gronlund et al. 2014). In terms of accessibility to health and cooling infrastructure, in the \geq 5-out-of-6 and 4-out-of-6 categories

(Figure 2.1a and 2.1b) all DAs were within the distance thresholds for all infrastructural variables.

When the 3-out-of-6 category is examined, one DA falls outside the distance thresholds for cool shelters and the rapid transit network (Figure 2.2a). This DA is 2700 metres from the closest rapid transit station, and 1475 and 1100 metres from the closest community centre and library, respectively. With 8% of the population aged 65–74 years, 5% aged 0–4 years, and a median annual after-tax income for persons 15 years and older of \$22,800, this DA is in the top 25% vulnerability groups for elderly, infants, and income. The average values for Vancouver are 6% for elderly, 4% for infants, and a median annual after-tax income for persons 15 years and older of \$24,100.

When the 2-out-of-6 category is examined, two additional DAs fall outside the distance threshold for cool shelters, the rapid transit network, and also for drinking fountains (Figure 2.2b). For polygons 2 and 3 in Figure 2.2b, the distances from the closest cooling infrastructures are as follows: 1050 and 1020 metres from a community centre, 600 and 560 metres from a drinking fountain, 1020 and 1300 metres from a library, and 2285 and 1860 metres from a rapid transit station. These two DAs are in the top 25% groups for elderly (7% of the population) and infants (5% of the population).

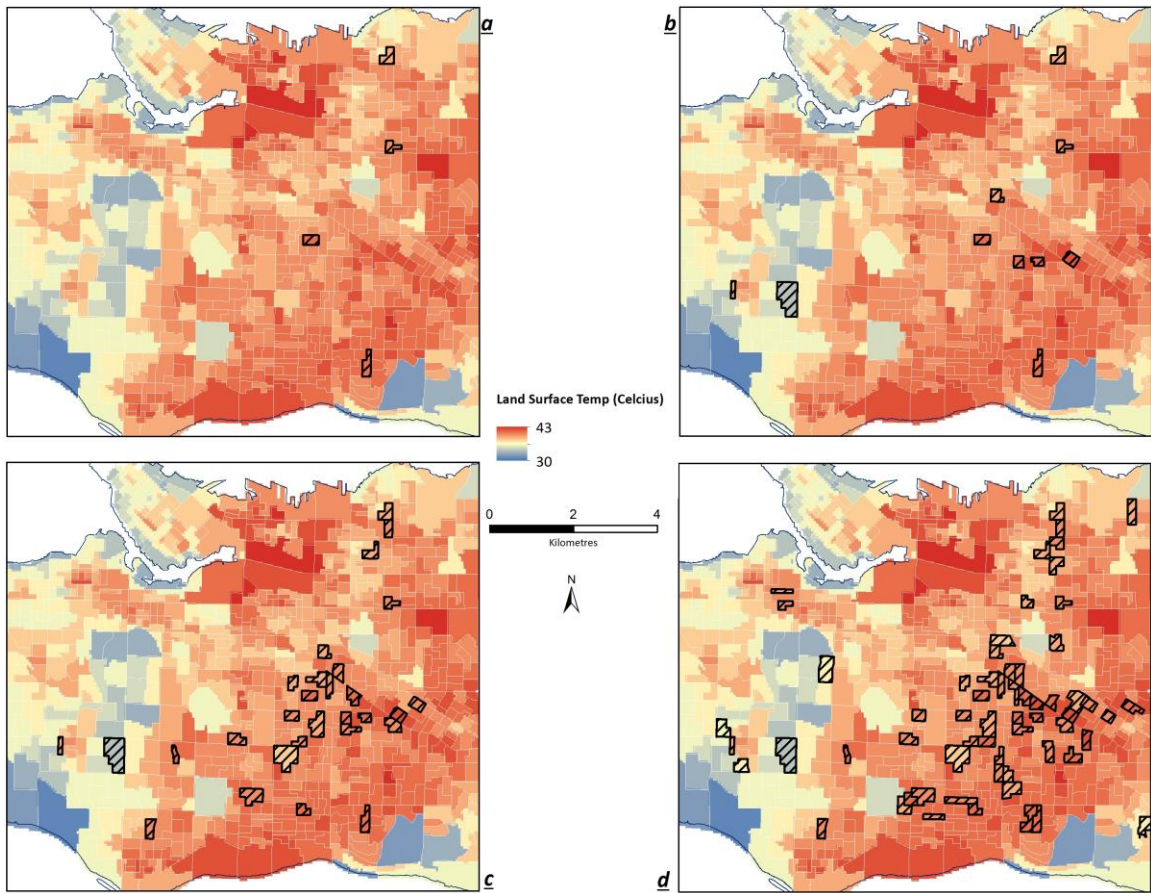


Figure 2-1: Polygons represent DAs in the top 25% most vulnerable areas for one or more indicators. Each map highlights DAs based on the number of co-existing vulnerability indicators—those in the top 25% for: (a) at least 5 out of 6 indicators; (b) 4 out of 6 indicators; (c) 3 out of 6 indicators; and (d) 2 out of 6 indicators. Map background shows spatial variations in land surface temperature.

The three vulnerable DAs highlighted here also have relatively low vegetation cover (NDVI average of three DAs: 0.08, Vancouver average: 0.15). They also have relatively hot surface temperatures (average of three DAs: 41 °C, Vancouver average: 38 °C). As such, they are socio-economically vulnerable, far from cooling and health infrastructure, and have an environment that elevates heat exposure. They are all located in the Sunset neighbourhood of southeast Vancouver, one of the most ethnically diverse, working class-dominated areas in the city (City of Vancouver 2016).

2.4. Discussion

Although these maps enable easy visual interpretation and a clear illustration of the distributions of a variety of heat vulnerability factors, the analyses are best viewed as preliminary, pointing to areas where more in-depth investigation is warranted, and where implementation of heat mitigation measures for vulnerable groups should be prioritized. The data should thus be used in conjunction with contextual knowledge of the area, other datasets that are either not publicly accessible or cannot be easily mapped, and wider discussions with relevant decision makers (Arup 2014). For example, homelessness in Vancouver has increased nearly three-fold in the last 10 years, from 628 individuals in 2002 to 2223 in 2019 (City of Vancouver 2019), but due to a lack of sufficient spatial data on this homelessness, information on this vulnerable population is excluded from this study. The inclusion of such information, as well as data on other highly vulnerable groups (e.g., those with alcohol or drug addictions as well as the mentally or physically disabled) would greatly assist in detection of vulnerable areas that may have been missed in the above analysis.

With regard to the issue of accessibility to cool shelters, drinking fountains, hospitals, and the rapid transit network, the hard thresholds (i.e., buffer distances) that were chosen provide some information but likely do not optimally describe the accessibility to city amenities. An alternative would have been to use network distance, but the best definition of the network is not clear in our case. Road networks are often used for this purpose, but people in high vulnerability groups seeking cooling on a hot summer day do not necessarily drive a car and may use alternatives to the road network for their travel, which complicates the calculation of realistic network distances. For exploratory purposes, we therefore chose the simpler and more easily interpretable buffer distance. Generally, the accessibility of a point or piece of land is a relative quality whose value is assigned based on the relationship of the point or piece of land with “the system of opportunities” (Fuglsang et al. 2011, 208), particularly those to be found in urban centres. This approach allows all locations to have a degree of relative accessibility (Ingram 1971). Accessibility varies as a function of distance to the destination: locations that are farthest from the destination have the lowest relative accessibility. Representing relative accessibility by the distance to city amenities is a subjective measurement yet is the simplest indicator of accessibility one can employ (Comber et al. 2008).

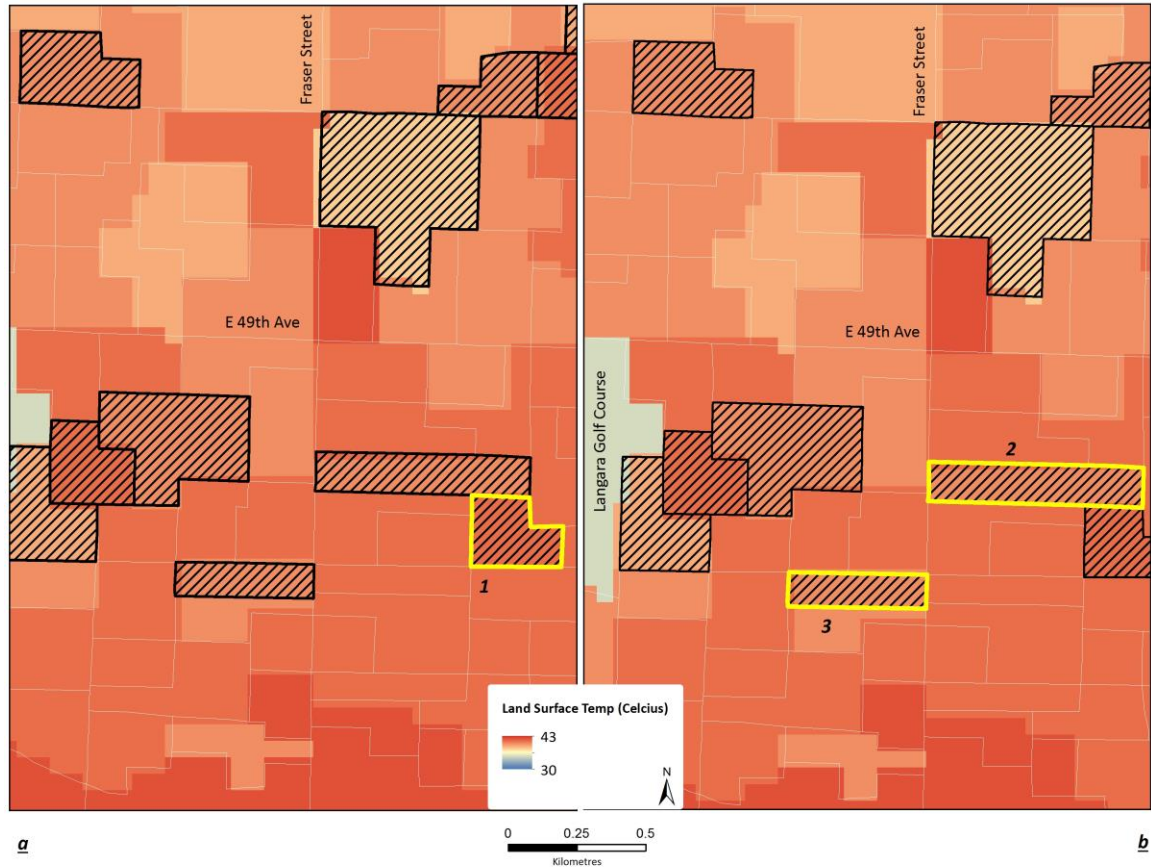


Figure 2-2: Polygons 1, 2, and 3 indicate vulnerable DAs far from health/cooling infrastructure. (a) This map represents the 3-out-of-6 category. Polygon 1 falls outside the distance thresholds for cool shelters and the rapid transit network. (b) This map represents the 2-out-of-6 category. Polygons 2 and 3 fall outside the distance thresholds for cool shelters, drinking fountains, and the rapid transit network.

Where data are available, mapping neighbourhood-level heat vulnerability can assist cities in targeting their resources effectively both immediately during heat emergencies and in the longer term through the incorporation of targeted heat mitigation measures in urban planning. The expectation that extreme heat events will increase in frequency and severity in the future means that heat should remain a prominent issue in local mitigation planning, including at the urban level (Bumbaco et al. 2013).

Our approach is largely qualitative and exploratory, visualizing overlays of multiple disparate socio-economic, environmental, and infrastructural datasets (Table 2.2) rather than attempting a quantitative integration for which sufficient calibration data and methodology do not exist. While the risk of living in a particularly vulnerable DA thus cannot be assessed, it is

clear that the combination of multiple socio-economic, environmental, and infrastructural vulnerability factors in some DAs constitutes a real concentration of risk. While only Vancouver neighbourhoods were investigated here, the methodology is easily transferable to other cities in Canada.

2.5. Conclusion

Extreme heat events can occur in any Canadian city, and with climate change, these events are forecasted to increase in frequency, length, and magnitude (Health Canada 2011a, 2011b). The overlay of multiple disparate spatial and population demographic data—socio-economic, environmental, and infrastructural—has facilitated the mapping of populations vulnerable to extreme heat in Vancouver. Using this spatial overlay analysis, dissemination areas that are particularly vulnerable have been identified within the city.

One of the strengths of this work is the ability to produce readily available information about heat vulnerability status. The approach taken in this study can be considered a first step toward the development of tools that can help health authorities, city officials, and policymakers better understand who is at risk during extreme heat events, where these people reside, and what factors drive their local risk. By understanding this multi-faceted context, both short-term emergency management efforts and longer-term urban planning interventions to reduce health effects of extreme heat events can be implemented with greater effectiveness.

2.6. Acknowledgements

The authors of this article gratefully acknowledge the City of Vancouver, Health Canada, and the Pacific Institute for Climate Solutions for supporting this research.

2.7. References

Alcoforado, M. J., D. Marques, R. A. C. Garcia, P. Canario, M. F. Nunes, H. Nogueira, and A. Cravosa. 2015. "Weather and climate versus mortality in Lisbon (Portugal) since the 19th century." *Applied Geography*. 57: 133–141.

- Anderson, B. G., and M. L. Bell. 2009. "Weather-related mortality: How heat, cold, and heat waves affect mortality in the United States." *Epidemiology*. 20 (2): 205–213.
- Anniballe, R., S. Bonafoni, and M. Pichierri. 2014. "Spatial and temporal trends of the surface and air heat island over Milan using MODIS data." *Remote Sensing of Environment*. 150: 163–171.
- Arup. 2014. Reducing urban heat risk: A study on urban heat risk mapping and visualization. London: Arup.
- Barriopedro, D., E. M. Fischer, J. Luterbacher, R. M. Trigo, and R. García-Herrera. 2011. "The hot summer of 2010: Redrawing the temperature record map of Europe." *Science*. 332 (6026): 220–224.
- Basu, R. 2009. "High ambient temperature and mortality: A review of epidemiologic studies from 2001 to 2008." *Environmental Health*. 8 (1): 1–13.
- Belanger, D., P. Gosselin, P. Valois, and B. Abdous. 2015. "Neighbourhood and dwelling characteristics associated with the self-reported adverse health effects of heat in most deprived urban areas: A cross-sectional study in 9 cities." *Health & Place*. 32: 8–18.
- Bouchama, A., M. Dehbi, G. Mohamed, F. Matthies, M. Shoukri, and B. Menne. 2007. "Prognostic factors in heat wave-related deaths: A meta-analysis." *Archives of Internal Medicine*. 167 (20): 2170–2176.
- Braga, L., A. Zanobetti, and J. Schwartz. 2001. "The time course of weather-related deaths." *Epidemiology*. 12 (6): 662–667.
- Bumbaco, K. A., K. D. Dello, and N. A. Bond. 2013. "History of Pacific Northwest heat waves: Synoptic pattern and trends." *Journal of Applied Meteorology and Climatology*. 52 (7): 1618–1631.
- Buscail, C., E. Upegui, and J. F. Viel. 2012. "Mapping heatwave health risk at the community level for public health action." *International Journal of Health Geographics*. 11: 38.
- Canoui-Poitrine, F., E. Cadot, and A. Spira. 2006. "Excess deaths during the August 2003 heat wave in Paris, France." *Revue d'Épidémiologie et de Santé Publique*. 54 (2): 127–135.
- Chestnut, L. G., W. S. Breffle, J. B. Smith, and L. S. Kalkstein. 1998. "Analysis of differences in hot-weather-related mortality across 44 U.S. metropolitan areas." *Environmental Science & Policy*. 1 (1): 59–70.
- Citro, C. F., M. Martin, and M. L. Straf, eds. 2009. Principles and practices for a federal statistical agency. 5th edition. Washington, DC: The National Academies Press.
- City of Vancouver. 2019. A home for everyone: Vancouver's housing and homelessness strategy, 2012–2021. Vancouver, BC: City of Vancouver.

- City of Vancouver. 2012. Climate change adaptation strategy. Vancouver, BC: City of Vancouver. <http://vancouver.ca/green-vancouver/climate-change-adaptation-strategy.aspx>.
- City of Vancouver. 2015. Open Data Catalogue. Vancouver, BC: City of Vancouver. <http://data.vancouver.ca/datacatalogue/index.htm>.
- City of Vancouver. 2016. About Vancouver: Sunset Area. <http://vancouver.ca/news-calendar/sunset.aspx>.
- Coates, L., K. Haynes, J. O'Brien, J. McAneney, and F. D. de Oliveira. 2014. "Exploring 167 years of vulnerability: An examination of extreme heat events in Australia 1844–2010." *Environmental Science & Policy*. 42: 33–44.
- Comber, A., C. Brunsdon, and E. Green. 2008. "Using a GIS-based network analysis to determine urban greenspace accessibility for different ethnic and religious groups." *Landscape and Urban Planning*. 86 (1): 103–114.
- Curriero, F. C., K. S. Heiner, J. M. Samet, S. L. Zeger, L. Strug, and J. A. Patz. 2002. "Temperature and mortality in 11 cities of the eastern United States." *American Journal of Epidemiology*. 155 (1): 80–87.
- Cutter, S. L., L. Barnes, M. Berry, C. Burton, E. Evans, E. Tate, and J. Webb. 2008. "A place-based model for understanding community resilience to natural disasters." *Global Environmental Change*. 18 (4): 598–606.
- Cutter, S. L., G. B. Christopher, and T. E. Christopher. 2010. "Disaster resilience indicators for benchmarking baseline conditions." *Journal of Homeland Security and Emergency Management*. 7 (1): 1–22.
- Depietri, Y., T. Welle, and F. G. Renaud. 2013. "Social vulnerability assessment of the Cologne urban area (Germany) to heat waves: Links to ecosystem services." *International Journal of Disaster Risk Reduction*. 6: 98–117.
- Dimoudi, A., and M. Nikolopoulou. 2003. "Vegetation in the urban environment: Microclimatic analysis and benefits." *Energy and Buildings*. 35 (1): 69–76.
- Dugord, P. A., S. Lauf, C. Schuster, and B. Kleinschmit. 2014. "Land use patterns, temperature distribution, and potential heat stress risk—The case study Berlin, Germany." *Computers, Environment and Urban Systems*. 48: 86–98.
- Fouillet, A., G. Rey, F. Laurent, G. Pavillon, S. Bellec, C. Guihenneuc-Jouyau, J. Clavel, E. Jougl, and D. Hémon. 2006. "Excess mortality related to the August 2003 heat wave in France." *International Archives of Occupational and Environmental Health*. 80 (1): 16–24.
- Fuglsang, M., H. S. Hansen, and B. Münier. 2011. Accessibility analysis and modelling in public transport networks—A raster-based approach. In *Computational Science and Its Applications—ICCSA 2011: International Conference Proceedings, Part I*, ed. B. Murgante, O. Gervasi, A. Iglesias, D. Taniar, and B. O. Apduhan. Berlin, Heidelberg: Springer-Verlag Berlin Heidelberg, 207–224.

- García-Herrera, R., J. Díaz, R. M. Trigo, J. Luterbacher, and E. M. Fischer. 2010. "A review of the European summer heat wave of 2003." *Critical Reviews in Environmental Science and Technology*. 40 (4): 267–306.
- Grize, L., A. Huss, O. Thommen, C. Schindler, and C. Braun-Fahrlander. 2005. "Heat wave 2003 and mortality in Switzerland." *Swiss Medical Weekly*. 135(13–14): 200–205.
- Gronlund, C. J., V. J. Berrocal, J. L. White-Newsome, K. C. Conlon, and M. S. O'Neill. 2014. "Vulnerability to extreme heat by socio-demographic characteristics and area green space among the elderly in Michigan, 1990–2007." *Environmental Research*. 136: 449–461.
- Harlan, S. L., A. J. Brazel, L. Prashad, W. L. Stefanov, and L. Larsen. 2006. "Neighborhood microclimates and vulnerability to heat stress." *Social Science & Medicine*. 63 (11): 2847–2863.
- Harlan, S. L., J. H. Deplet-Barreto, W. L. Stefanov, and D. B. Petitti. 2013. "Neighborhood effects on heat deaths: Social and environmental predictors of vulnerability in Maricopa County, Arizona." *Environmental Health Perspectives*. 121 (2): 197–204.
- Health Canada. 2011a. Communicating the health risks of extreme heat events: Toolkit for public health and emergency management officials. Ottawa, ON: Health Canada.
- Health Canada. 2011b. Adapting to extreme heat events: guidelines for assessing health vulnerability. Ottawa, ON: Health Canada.
- Henderson, S. B., V. Wan, and T. Kosatsky. 2013. "Differences in heat-related mortality across four ecological regions with diverse urban, rural, and remote populations in British Columbia, Canada." *Health & Place*. 23: 48–53.
- Ho, H. C., A. Knudby, and W. Huang. 2015. "A spatial framework to map heat health risks at multiple scales." *International Journal of Environmental Research and Public Health*. 12 (12): 16110–16123.
- Ho, H. C., A. Knudby, P. Sirovyak, Y. Xu, M. Hodul, and S. B. Henderson. 2014. "Mapping maximum urban air temperature on hot summer days." *Remote Sensing of Environment*. 154: 38–45.
- Hondula, D. M., R. E. Davis, M. V. Saha, C. R. Wegner, and L. M. Veazey. 2015. "Geographic dimensions of heat-related mortality in seven U.S. cities." *Environmental Research*. 138: 439–452.
- Imhoff, M. L., P. Zhang, R. E. Wolfe, and L. Bounoua. 2010. "Remote sensing of the urban heat island effect across biomes in the continental USA." *Remote Sensing of Environment*. 114 (3): 504–513.
- Ingram, D. R. 1971. "The concept of accessibility: A search for an operational form." *Regional Studies*. 5 (2): 101–107.

- IOM (Institute of Medicine). 2009. Race, ethnicity, and language data: Standardization for health care quality improvement. Washington, DC: The National Academies Press.
- IPCC (Intergovernmental Panel on Climate Change). 2014. Climate Change 2014: Synthesis Report. Contribution of Working Groups I, II and III to the Fifth Assessment Report of the Intergovernmental Panel on Climate Change. Geneva, Switzerland: IPCC.
- Isaksen, T. M. B. 2014. Extreme heat events and associated health outcomes in King County, WA: A study of historical outcomes, model validation, and heat-risk mapping. PhD Thesis, Department of Environmental and Occupational Health Sciences, University of Washington.
- Jackson, J. E., M. G. Yost, C. Karr, C. Fitzpatrick, B. Lamb, S. Chung, J. Chen, J. Avise, R. Rosenblatt, and R. Fenske. 2010. "Public health impacts of climate change in Washington State: Projected mortality risks due to heat events and air pollution." *Climatic Change*. 102 (1–2): 159–186.
- Jones, T., A. P. Liang, E. M. Kilbourne, M. R. Griffin, P. A. Patriarca, S. G. Fite Wassailak, R. J. Mullan, et al. 1982. "Morbidity and mortality associated with the July 1980 heat wave in St Louis and Kansas City". *The Journal of the American Medical Association*. 247 (24): 3327–3331.
- Keller, R. C. 2013. "Place matters: Mortality, space, and urban form in the 2003 Paris heat wave disaster." *French Historical Studies*. 36 (2): 299–330.
- Kilbourne, E. M., K. Choi, T. Jones, and S. B. Thacker. 1982. "Risk factors for heatstroke: A case-control study." *Journal of the American Medical Association*. 247 (24): 3332–3336.
- Klinenberg, E. 1999. "Denaturalizing disaster: A social autopsy of the 1995 Chicago heat wave." *Theory and Society*. 28 (2): 239–295.
- Knowlton, K., J. E. Rosenthal, C. Hogrefe, B. Lynn, S. Gaffin, R. Goldberg, C. Rosenzweig, K. Civerolo, J. Y. Ku, and P. L. Kinney. 2004. "Assessing ozone-related health impacts under a changing climate." *Environmental Health Perspectives*. 112 (15): 1557–1563.
- Knowlton, K., M. Rotkin-Ellman, G. King, H. G. Margoli, D. Smith, G. Soloman, R. Trent, and P. English. 2009. "The 2006 California heat wave: impacts on hospitalizations and emergency department visits." *Environmental Health Perspectives*. 117 (1): 61–67.
- Kosatsky, T., S. B. Henderson, and S. L. Pollock. 2012. "Shifts in mortality during a hot weather event in Vancouver, British Columbia: Rapid assessment with case-only analysis." *American Journal of Public Health*. 102 (12): 2367–2371.
- Kosatsky, T., N. King, and B. Henry. 2005. How Toronto and Montreal (Canada) respond to heat. In *Extreme weather events and public health responses*, ed. W. Kirch, R. Bertollini, and B. Menne. Berlin: Springer Berlin Heidelberg, 167–171.

- Loughnan, M., N. Tapper, and T. Phan. 2014. "Identifying vulnerable populations in subtropical Brisbane, Australia: A guide for heatwave preparedness and health promotion." *ISRN Epidemiology*. 2014: 821759.
- Loughnan, M., N. Tapper, T. Phan, K. Lynch, and J. A. McInnes. 2013. A spatial vulnerability analysis of urban populations during extreme heat events in Australian capital cities. Southport, Australia: National Climate Change Adaptation Research Facility.
- Luber, G., C. Sanchez, and L. Conklin. 2006. "Heat-related deaths in United States, 1999–2003." *Morbidity and Mortality Weekly Report*. 55 (29): 796–798.
- Luers, A. L., D. B. Lobell, L. S. Sklar, C. L. Addams, and P. A. Matson. 2003. "A method for quantifying vulnerability, applied to the agricultural system of the Yaqui Valley, Mexico." *Global Environmental Change*. 13 (4): 255–267.
- Malone, E., and A. Brenkert. 2008. "Uncertainty in resilience to climate change in India and Indian states." *Climatic Change*. 91 (3): 451–476.
- Mastrangelo, G., U. Fedeli, C. Visentin, G. Milan, E. Fadda, and P. Spolaore. 2007. "Pattern and determinants of hospitalization during heat waves: An ecologic study." *BioMedCentral Public Health*. 7 (1): 1–8.
- Medina-Ramón, M., A. Zanobetti, D. P. Cavanagh, and J. Schwartz. 2006. "Extreme temperatures and mortality: Assessing effect modification by personal characteristics and specific cause of death in a multi-city case-only analysis." *Environmental Health Perspectives*. 114 (9): 1331–1336.
- Meehl, G. A., and C. Tebaldi. 2004. "More intense, more frequent, and longer lasting heat waves in the 21st century." *Science*. 305 (5686): 994–997.
- Naughton, M. P., A. Henderson, M. C. Mirabelli, R. Kaiser, J. L. Wilhelm, S. M. Kieszak, C. H. Rubin, and M. A. McGeehin. 2002. "Heat-related mortality during a 1999 heat wave in Chicago." *American Journal of Preventive Medicine*. 22 (4): 221–227.
- O'Neill, M. S., A. Zanobetti, and J. Schwartz, eds. 2003. "Modifiers of the temperature and mortality association in seven US cities." *American Journal of Epidemiology*. 157 (12): 1074–1082.
- Onozuka, D., and A. Hagihara. 2015. "Variation in vulnerability to extreme-temperature-related mortality in Japan: A 40-year time-series analysis." *Environmental Research*. 140: 177–184.
- Papanastasiou, D. K., D. Melas, and H. D. Kambezidis. 2015. "Air quality and thermal comfort levels under extreme hot weather." *Atmospheric Research*. 152: 4–13.
- Pengelly, L. D., M. E. Campbell, C. S. Cheng, C. Fu, S. E. Gingrich, and R. Macfarlane. 2007. "Anatomy of heat waves and mortality in Toronto: Lessons for public health protection." *Canadian Journal of Public Health*. 98 (5): 364–368.

- Price, K., S. Perron, and N. King. 2013. "Implementation of the Montreal heat response plan during the 2010 heat wave." *Canadian Journal of Public Health*. 104 (2): 96–100.
- Public Safety Canada. 2013. Canadian Disaster Database. <http://cdd.publicsafety.gc.ca/>
- Reid, C. E., M. S. O'Neill, C. J. Gronlund, S. J. Brines, D. G. Brown, A. V. Diez-Roux, and J. Schwartz. 2009. "Mapping community determinants of heat vulnerability." *Environmental Health Perspectives*. 117 (11): 1730–1736.
- Rinner, C., D. Patychuk, K. Bassil, S. Nasr, S. Gower, and M. Campbell. 2013. "The role of maps in neighborhood-level heat vulnerability assessment for the City of Toronto." *Cartography and Geographic Information Science*. 37 (1): 31–44.
- Rizwan, A. M., L. Dennis, and C. Liu. 2008. "A review on the generation, determination and mitigation of urban heat island." *Journal of Environmental Sciences*. 20 (1): 120–128.
- Robine, J. M., S. L. K. Cheung, S. L. Roy, H. Van Oyen, C. Griffiths, J. P. Michel, and F. R. Herrmann. 2008. "Death toll exceeded 70,000 in Europe during the summer of 2003." *Comptes Rendus Biologies*. 331 (2): 171–178.
- Rosenthal, J. K., P. L. Kinney, and K. B. Metzger. 2014. "Intra-urban vulnerability to heat-related mortality in New York City, 1997–2006." *Health & Place*. 30: 45–60.
- Saha, M. V., R. E. Davis, and D. M. Hondula. 2014. "Mortality displacement as a function of heat event strength in 7 US cities." *American Journal of Epidemiology*. 179 (4): 467–474.
- Schuster, C., K. Burkart, and T. Lakes. 2014. "Heat mortality in Berlin: Spatial variability at the neighborhood scale." *Urban Climate*. 10 (Part 1): 134–147.
- Semenza, J. C., C. H. Rubin, K. H. Falter, J. C. Selanikio, D. Flanders, H. L. Howe, and J. L. Wilhelm. 1996. "Heat-related deaths during the July 1995 heat wave in Chicago." *New England Journal of Medicine*. 335 (2): 84–90.
- SFDPH (San Francisco Department of Public Health). 2013. Climate and health: An assessment of San Francisco's vulnerability to extreme heat events. San Francisco, CA: San Francisco Department of Public Health.
- Sheridan, S. C. 2007. "A survey of public perception and response to heat warnings across four North American cities: An evaluation of municipal effectiveness." *International Journal of Biometeorology*. 52 (1): 3–15.
- Smoyer, K. E. 1998. "Putting risk in its place: Methodological considerations for investigating extreme event health risk." *Social Science & Medicine*. 47 (11): 1809–1824.
- Statistics Canada. 2006. Census of Population. <http://www12.statcan.ca/census-recensement/2006/index-eng.cfm>.
- Statistics Canada. 2015. Census Dictionary. <https://www12.statcan.gc.ca/census-recensement/2011/ref/dict/geo021-eng.cfm>.

- Vandentorren, S., P. Bretin, A. Zeghnoun, L. Mandereau-Bruno, A. Croisier, C. Cochet, J. Ribéron, I. Siberan, B. Declercq, and M. Ledrans. 2006. "August 2003 heat wave in France: Risk factors for death of elderly people living at home." *The European Journal of Public Health*. 16 (6): 583–591.
- Zhang, K., Y. Li, J. D. Schwartz, and M. S. O'Neill. 2014. "What weather variables are important in predicting heat-related mortality? A new application of statistical learning methods." *Environmental Research*. 132: 350–359.

Chapter 3. Modelling the impact of increased street tree cover on mean radiant temperature across Vancouver’s local climate zones

This chapter has been published in the Urban Forestry and Urban Greening journal.

Citation details: Aminipouri, M., Knudby, A., Krayenhoff, E.S., Zickfeld, K., and Middel, A., 2019. “Modelling the impact of increased street tree cover on mean radiant temperature across Vancouver’s local climate zones.” Urban Forestry and Urban Greening 39, 9-17.

Contribution statement: First author outlined the research idea with support from Dr. Anders Knudby and Dr. Kirsten Zickfeld, designed the simulations with support from Dr. Ariane Middel and Dr. Scott Krayenhoff, performed the analysis and wrote the manuscript. All co-authors provided feedback and edited the manuscript.

3.1. Abstract

Extensive impervious surface cover, anthropogenic heat emissions, and lack of vegetation contribute to the formation of distinct urban microclimates where higher air and surface temperature as well as lack of shade intensify outdoor heat exposure and thermal discomfort for humans. Modifications to the thermal environment via urban design can be used to mitigate this effect. In this study, the potential for increased street tree coverage to reduce mean radiant temperature (T_{mrt}) across six different local climate zones (LCZs) in Vancouver, Canada, was examined using the SOLar and LongWave Environmental Irradiance Geometry (SOLWEIG) model. The radiant cooling effect of increased street tree coverage during the hottest day on record for Vancouver (July 29, 2009) was quantified by spatiotemporal changes to T_{mrt} . SOLWEIG was evaluated successfully prior to implementation of a street tree cover increase equivalent to 1% of plan area in each of six Vancouver LCZs investigated. Results indicate 3.2–6.3 °C reduction in spatially-averaged daytime (9:00 – 18:00) T_{mrt} and 3.3–7.1 °C reduction during the hottest period of day, 11:00-17:00. During the hottest period of day, the

largest spatially-averaged T_{mrt} reduction (7.1 °C) was modelled in a low-rise residential area. Modelling suggested that a pedestrian standing directly under a tree canopy would experience T_{mrt} reductions of 15.5–17.3 °C in all LCZs. Also, under current conditions with no increase in tree cover, the compact high-rise and the large low-rise areas are shown to be the most and least comfortable environments regarding human thermal exposure with spatially-averaged T_{mrt} of 41.9 °C and 47.9 °C, respectively. We conclude that increases to Vancouver’s street tree cover by 1% of plan area can substantially reduce T_{mrt} during extreme hot weather. The results of this study show that the cooling potential of added street trees is greater in lower density residential neighborhoods with 1–2 storey buildings compared to higher density neighborhoods occupied by high-rise or mid-rise buildings.

Keywords: Mean radiant temperature, Micrometeorological modelling, SOLWEIG, Urban greening

3.2. Introduction

The world has seen an ever-increasing trend in the population of urban dwellers. Urban centers are becoming the dominant setting for world’s population. By 2030, more than 60% of the world population is predicted to reside in urban centers (World Cities Report, United Nations, 2016). Extensive increase in impervious surfaces, large amounts of heat emissions, and lack of urban greenery causes excessive heat storage, reduction in substrate moisture content, and consequently reduction of latent heat fluxes from evaporation and transpiration processes (Asaeda et al., 1996; Salata et al., 2015). Local wind is another factor affected by the complexity of urban environments. Urban canyons with less exposure to wind can experience reduced convective heat loss (Erell et al., 2011). These ultimately contribute to the formation of distinct urban microclimates where higher air and surface temperature can intensify outdoor heat exposure and thermal discomfort for pedestrians (Thom et al., 2016). Extensive exposure to extreme heat has also shown to negatively affect human’s physiological comfort, leading to severe heat vulnerability, stress and heat-related mortality and morbidity (Aminipouri et al., 2016; Luber et al., 2006; Reid et al., 2009). As an example, the July 2009 heatwave in Vancouver and exposure to high air temperature of 34°C for a week, caused an estimated 122 excess deaths (Kosatsky et al., 2012).

Human thermal exposure is affected directly by the radiative heat exchange between the human body and its surroundings. In this regard, both environmental and personal factors play critical roles. Factors such as air temperature, relative humidity and wind speed, direct and diffuse shortwave and longwave radiant fluxes as well as clothing insulation and metabolic rate need to be considered for assessing heat exposure and thermal comfort (Mayer 1993). Human thermal exposure is particularly variable in cities (Hondula et al. 2017), where shade and surface temperature can vary substantially over very short distances. Identifying key factors that affect T_{mrt} directs the attention of research to possible heat mitigation measures, including but not limited to, urban morphology alteration, surface and building materials modifications, building insulation and urban greenery inclusion (Akbari et al., 2001; Akbari and Konopacki, 2005; Middel et al., 2014; Middel et al., 2015; Morakinyo and Lam, 2016; Santamouris, 2014; Zölch et al., 2016).

A synthetic human-biometeorological quantity that has been found to be a major driver of thermal exposure is the mean radiant temperature T_{mrt} (Chen et al., 2016; Jänicke et al., 2016; Lau et al., 2016). T_{mrt} is defined as the sum of all shortwave and longwave radiation fluxes from six directions (four cardinal, one from below and one from above) applied to a reference pedestrian (Höppe, 1992). Of particular interest to thermal exposure studies is the effect of street trees on reducing T_{mrt} through the provision of shade (Holst and Mayer 2011; Lee et al., 2016; Lee, Holst, and Mayer 2013; Lee and Mayer 2018; Lee, Mayer, and Schindler 2014; Lobaccaro and Acero, 2015; Mayer et al. 2008; Middel et al., 2016).

The mitigating effect of street trees on diurnal mean T_{mrt} has been widely investigated. T_{mrt} reductions ranged from 7°C in a residential district in Freiburg, Germany (Lee et al., 2016) to 10°C in a compact low-rise neighborhood in Bilbao, Spain (Lobaccaro and Acero, 2015). All measurements were conducted for 24 hours period under calm sunny days in summer. Another study in Berlin, Germany, evaluated the effect of façade greening on T_{mrt} (Jänicke et al., 2015). The study examined the reduction of T_{mrt} in front of a green façade in a hot day in July 2013, using three different models: SOLWEIG (V 2013a), ENVI-met (V 3.1 Beta 5) and RayMan (V 1.2). Comparing modelled vs observed T_{mrt} , SOLWEIG showed the highest agreement ($R^2=0.96$) and lowest root mean square deviation (RMSD=4.63 °C).

SOLWEIG has been validated and shown to accurately predict T_{mrt} across cities with various climates such as Gothenburg, Sweden (Thorsson et al., 2011), London, England (Lindberg and Grimmond, 2011a), Freiburg, Germany (Chen et al., 2014), Adelaide, Australia (Thom et al., 2016), Shanghai, China (Chen et al., 2016) and Hong Kong (Lau et al., 2016).

To date, most of the thermal exposure studies have focused on heat mitigation strategies to reduce T_{mrt} over single point locations (Martins et al., 2016; Taleghani et al., 2014). However, there has been little research into how the local environment influences the effectiveness of such heat mitigation strategies, and thus how their effectiveness differs between LCZs within a city. Environmental factors that influence such effectiveness include those that impact local energy fluxes, such as surface albedo, building height, density and materials, vegetation cover and its spatial arrangement, and anthropogenic heat sources.

The LCZ approach introduced by Stewart and Oke (2012) categorizes landscapes into ten urban classes, seven non-urban classes, and a range of mixed classes based on their impact on the screen-level air temperature. LCZs are defined by their surface properties (e.g. albedo, height-to-width ratio, sky view factor, tree and building height), which are measurable and independent of time or space (Stewart and Oke, 2012). Such class definition makes the LCZ approach a useful classification system for studying how the effectiveness of different heat mitigation strategies depends on the local environment, and ultimately facilitates knowledge transfer between urban climatologists, planners and practitioners (Alexander et al., 2016).

The main research questions here are twofold: (a) Under current conditions, which LCZ provides the most and which one provides the least comfortable thermal environment for humans in terms of T_{mrt} variations? and (b) How much will the spatial average T_{mrt} change if tree cover is increased by 1% of the total plan area for different LCZs?

This study seeks to assess the current spatiotemporal variation of T_{mrt} and its daytime reductions resulting from increased tree cover within street sections of representative LCZs in Vancouver, Canada. Vancouver's urban forestry strategy (Urban Forestry Strategy, City of Vancouver, 2014) aims to grow its aerial urban canopy cover by 1% by the year 2020. The effect of a 1% increase in plan area tree coverage on T_{mrt} is therefore modeled using SOLWEIG (Lindberg and Grimmond, 2011b), for a scenario informed by the hottest day on record for Vancouver - July 29, 2009.

3.3. Materials and methods

3.3.1. Study area

Vancouver, Canada, located in the southwestern corner of the province of British Columbia (49.2°N, 123.1°W), has a moderate oceanic climate with annual mean air temperature of 14°C, mild winters and semi-dry summer months. The city is located on the coast of the Pacific Ocean, and includes areas ranging from the foothills of the North Shore Mountains to the Fraser River Valley and its floodplains in the south. Combined with the range of urban densities found in the area, this environmental context produces substantial differences in thermal environment between different parts of the city (Ho et al., 2016).

We selected a range of LCZs that were considered typical for Vancouver and for which data are available (current as of February 2013) to generate a building digital surface model (BDSM) and a tree digital surface model (TDSM) both of which are essential inputs in SOLWEIG. In total six LCZs were selected: compact high-rise (LCZ 1), open high-rise (LCZ 4), open mid-rise (LCZ 5), open low-rise (LCZ 6), open low-rise with dense trees (LCZ 6A), and large low-rise (LCZ 8). The sites were each approximately 300x300 m, with streets oriented east-west and north-south, or at approximately 45° to the cardinal directions (see Figure 3.1).

3.3.2. SOLWEIG

SOLWEIG is a 3D solar radiation modelling tool designed to estimate the variations of shortwave and longwave radiation fluxes, T_{mrt} , and shadow patterns (Lindberg and Grimmond, 2011b). SOLWEIG is computationally fast (e.g. 12 hours of computational time for a 350*350 m² complex urban area accompanied by 20 years of hourly weather data) (Thorsson et al., 2011), user-friendly and requires a limited number of inputs: BDSM, TDSM, and meteorological data such as air temperature (T_a), relative humidity (RH).

LCZs	Site Photographs		Site properties ¹	LCZ schematics ²
	Aerial view	Sky view		
LCZ 1			SVF 0.2 % built-up >95 Z _H 75-100	 Compact highrise
LCZ 4			SVF 0.5 % built-up 80 Z _H 50-75	 Open highrise
LCZ 5			SVF 0.55 % built-up 85 Z _H 15-30	 Open midrise
LCZ 6			SVF 0.75 % built-up 45-55 Z _H 5-10	 Open lowrise
LCZ 6A			SVF 0.7 % built-up 40-50 Z _H 7-15	 Open lowrise (dense trees)
LCZ 8			SVF 0.77 % built-up >95 Z _H 5	 Large lowrise

Figure 3-1: Aerial view and sky view of 6 LCZs in Vancouver. The study areas are: (a) LCZ 1 compact high-rise; (b) LCZ 4 open high-rise; (c) LCZ 5 open-mid-rise; (d) LCZ 6 open low-rise; (e) LCZ 6A open low-rise with dense trees; and (f) LCZ 8 large low-rise.

¹ Sky View Factor (SVF); % built-up= the sum of ground-level impervious and building surfaces fractions; Z_H=geometric average of building or plant-canopy heights (m). ² LCZ schematics are adopted from Stewart and Oke (2012).

To calculate T_{mrt} for a standing person at a height of 1.1 m exposed to the sun, the mean radiant flux (R) is calculated first. Mean radiant flux (R) is defined as the sum of all long (L_i) and shortwave (K_i) radiation from six directions: four cardinals (north, south, east and west) and upward and downward directions. Moreover, the angular factor (F), absorption coefficient ($1-\alpha$) and emissivity of the human body (ϵ_p) of an individual are considered:

$$R = 1 - \alpha \sum_{i=1}^6 K_i F_i + \epsilon_p \sum_{i=1}^6 L_i F_i$$

(Eq. 1)

- $F_i=0.22$ for radiation fluxes from the four cardinal directions and 0.06 for upward and downward radiation fluxes.
- $1-\alpha=0.7$ and $\epsilon_p=0.97$ (VDI 1994).

Then T_{mrt} in degree Celsius is calculated from R using the Stefan Boltzmann's law:

$$T_{mrt} = \sqrt[4]{\left(\frac{R}{\epsilon_p \sigma}\right)} + 273.15$$

(Eq. 2)

- σ is the Stefan Boltzmann constant ($5.67 * 10^{-8} \text{ Wm}^{-2}\text{K}^{-4}$)

A detailed description of the SOLWEIG model can be found in (Lindberg et al., 2008).

3.3.3. SOLWEIG evaluation

We evaluated the SOLWEIG model for each of the six sites by comparing measured T_{mrt} for multiple locations at each site to their SOLWEIG-modeled equivalents.

T_{mrt} was measured for one clear-sky day at each site by collecting surface air temperature (T_a), wind speed (v), RH and black globe temperature (T_g), from 9:00 to 18:00, using a Kestrel 4600 portable heat stress meter (Figure 3.2). Measurements were taken every 10

minutes, at different locations spanning each site, such as over grass, over asphalt or under a tree. The 10-minute interval allows the device to adapt itself to the new location every time it is moved. For all measurements, the Kestrel meter was mounted on a tripod at the height of 1.1 m, equivalent to the center of gravity for an average standing human.



Figure 3-2: Portable heat stress meter (Kestrel 4600) mounted at 1.1 m on a tripod used for the evaluation of simulated T_{mrt} values.

We then calculated observed T_{mrt} according to the equation below (Thorsson et al., 2007).

$$T_{mrt} = \left[(T_g + 273.15)^4 + \frac{1.1 \times 10^8 V_a^{0.6}}{\epsilon D^{0.4}} \times (T_g - T_a) \right]^{0.25} - 273.15$$

(Eq. 3)

- *T_g*: globe temperature (°C); *V_a*: air velocity (ms⁻¹); *T_a*: air temperature (°C); *D*: globe diameter (2.54 cm); *ε*: globe emissivity (0.95)

The empirical derived factor 1.1×10^8 and the wind exponent ($V_a^{0.6}$) together compute the globe's mean convection coefficient ($1.1 \times 10^8 V_a^{0.6}$). It is assumed that the calculation of T_{mrt} under Equation 3 is valid in conditions with wind speed ranging between 0.1 and 4.0 ms⁻¹ and incoming short-wave radiation ranging between 100 and 850 Wm⁻² and optimized for simple small-size portable globe thermometers such as the one used in this study (Thorsson et al., 2007).

We created high quality BDSMs and TDSMs with resolution of 0.3m from 0.3m-resolution light detection and ranging (LiDAR) data obtained from City of Vancouver's open data catalogue ("Open Data Catalogue, City of Vancouver," 2018). Based on field observations, we selected deciduous trees as an input for TDSMs. Tree height and location were derived from the LiDAR data, while trunk height and tree crown diameter were measured in the field.

The sub-hourly meteorological data required to run SOLWEIG, including air temperature (°C), relative humidity (%), and global incoming, direct and diffuse shortwave radiation (W m⁻²), were obtained from Environment Canada's weather station at Vancouver International Airport for the exact days when fieldwork was conducted. Default values for environmental parameters such as transmissivity of light through vegetation (3%) (Konarska et al., 2014), emissivity and albedo of wall (0.9, 0.2) and ground (0.95, 0.15) surfaces (Oke, 1988) were used in the model. T_{mrt} was then simulated every 10 minutes from 9:00-18:00 for each LCZ. We then examined the accuracy of SOLWEIG model using three different measures of model performance: the coefficient of determination (R^2), the mean absolute error (MAE) and the root mean square error (RMSE) (see Table 3.1).

Table 3-1: The correlation between measured and modelled T_{mrt} (°C) is shown for two time periods: all day (9:00-18:00) and hottest period of day (11:00-17:00). For each LCZ, R^2 , mean absolute error (MAE, °C) and root mean square error (RMSE, °C) are stated.

Location	All day (9:00 – 18:00)					Hottest Period of Day (11:00 – 17:00)				
	Measured		Modelled			Measured		Modelled		
	T_{mrt}	T_{mrt}	R^2	MAE	RMSE	T_{mrt}	T_{mrt}	R^2	MAE	RMSE
LCZ 1	34.1	37.1	0.91	3.96	5.36	34.6	37.7	0.88	3.10	4.44
LCZ 4	31.2	34.5	0.85	5.52	6.51	36.2	38.5	0.84	5.41	5.38
LCZ 5	34.2	36.5	0.92	3.10	4.71	38.6	41.4	0.82	2.81	3.73
LCZ 6	42.1	44.5	0.90	4.46	3.92	43.7	47.6	0.87	3.90	3.57
LCZ 6A	35.1	37.8	0.94	4.71	4.01	43.3	47.1	0.82	3.87	3.74
LCZ 8	38.5	41.9	0.89	3.44	6.87	40.2	43.4	0.78	3.24	6.08

3.3.4. Increased street tree scenario

Subsequently, the spatial distribution of T_{mrt} was modeled in SOLWEIG for each of the six study sites, based on meteorological data from July 29, 2009. The influence of the 1% plan area increase in street tree cover proposed in Vancouver’s Urban Forestry Strategy was then assessed by adding street trees to the input data for each site and re-running the model. Trees were added using the following considerations:

- The total tree canopy cover (i.e. number of tree pixels per surface cover) was calculated in percent for each LCZ. Then, the number of pixels required for 1% increase in tree canopy were computed.
- Due to very limited space on the sidewalks of each site, new trees were added adjacent to existing trees.
- Based on field observations and street tree data from Vancouver’s open data catalogue, deciduous trees with 4m crown diameter, 2.6m trunk height and 7m tree height, representing typical street trees in the city, were added.

- Since the spatial variations of T_{mrt} are assessed for each site, trees were added to all publicly accessible sidewalks regardless of street orientation.

The existing and added street trees for each LCZ are illustrated in Figure 3-3.

3.4. Results and discussion

3.4.1. Evaluation of SOLWEIG with field measurements

The correlation between measured and modelled T_{mrt} shows the performance of the SOLWEIG model is very good across all six LCZs, with R^2 values ranging from 0.85 to 0.94. The MAE values obtained during validation (3.10-5.52°C) are comparable to those from previous SOLWEIG studies, including a case study in Adelaide, Australia (Thom et al., 2016) where MAE ranges between 3.11-5.63°C across 5 different land covers; MAE of 3.48°C for modelling a single green wall in Germany (Jänicke et al., 2015); and MAE of 2.74°C for observations in Sweden and Germany (Lindberg and Grimmond, 2011b).

The evaluation results indicate that SOLWEIG-based T_{mrt} estimates are higher than the corresponding observations by approximately 2-3°C across all LCZs. Exposure of the black globe thermometer to wind and inconsistent shadow patterns are likely causes of the lower observed T_{mrt} values. MAE is decreased when only the hottest part of the day (11:00 - 17:00) is considered, compared to the full day (9:00 – 18:00). This could be because the zenith angle is smaller during the hottest part of the day, and therefore the measurement of $T_{g,r}$ and consequently the estimated T_{mrt} , is less affected by factors such as shadow patterns (Lindberg and Grimmond, 2011b). Based on the model evaluation results, it is concluded that SOLWEIG performs well and can accurately model local spatial variations of T_{mrt} for all six LCZs in Vancouver. It is worthwhile mentioning that the evaluation of SOLWEIG relates to the model's performance for average conditions in each LCZ, but not for specific surface types or local environmental contexts.

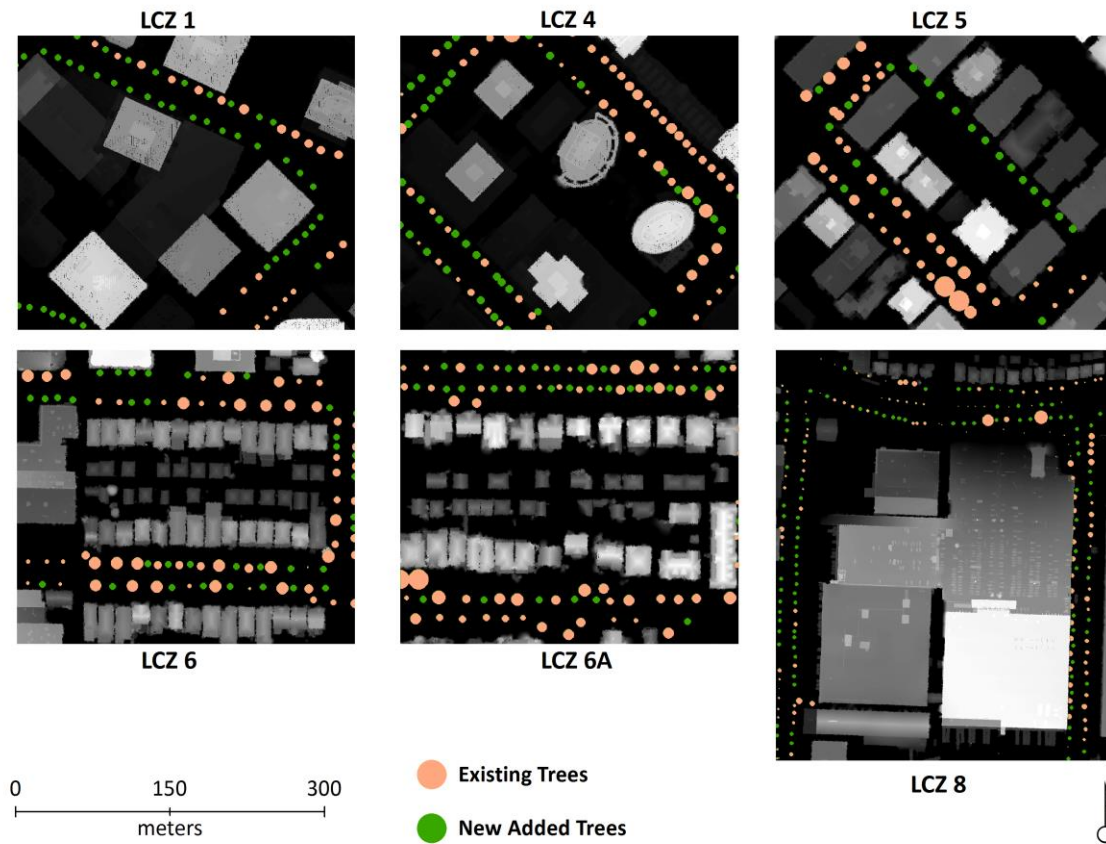


Figure 3-3: Existing and added street trees for the 1% increase in street tree cover scenarios, overlaid on the BDSMs at each LCZ.

3.4.2. Spatial patterns of T_{mrt}

Spatial variations of T_{mrt} across all six LCZs were mapped for July 29, 2009, the hottest day on record for Vancouver (Figure 3-4). The range for T_{mrt} is 35.0-54.4°C across all six LCZs. Under current land use and land cover configurations, LCZ 8 is the least comfortable LCZ with an average T_{mrt} of 47.9°C. This is caused primarily by lack of shading in the large low-rise LCZs, typical of suburban commercial areas where land is mostly covered by impervious surfaces such as huge parking lots. On the other hand, LCZ 1, with an average T_{mrt} of 41.9°C, is the most thermally comfortable environment for humans. This is primarily due to the extensive shadows cast by high-rise buildings in this environment, typical of downtown Vancouver. LCZ 4 comes with daily average T_{mrt} of 43.5°C, LCZ 5 with 45.1°C, LCZ 6 with 47.5°C and LCZ 6A with 47.2°C.

The intra-LCZ variability of T_{mrt} is approximately 10°C, which is reasonable considering the structural and environmental complexity of each LCZ with different sky view factors, geometries of buildings, tree shapes and sizes and street orientation, with various shadow patterns (Shashua-Bar et al., 2011; Srivanit and Hokao, 2013).

Within LCZs, the daytime average T_{mrt} varies slightly between different street orientations. For LCZ 8 for example, daily average T_{mrt} of 48.7°C was modelled for E-W sidewalks compared to that of 47.5°C for N-S sidewalks. In LCZ 1, these were reduced to 41.7°C and 40.2°C for NW-SE, SW-NE oriented sidewalks, respectively.

T_{mrt} variations were also examined temporally for all LCZs. It was found that for all LCZs T_{mrt} peaked at solar noon time, 12:00 pm, when the sun was at its maximum elevation. Slightly greater peak T_{mrt} values were observed in mixed-residential neighborhoods of LCZ 4 and LCZ 5 (60.4°C and 59.6°C), residential LCZ 6 (59.5°C) and 6A (58.5°C), and commercial LCZ 1 (58.5°C) than that of LCZ8. The large low-rise neighborhood of LCZ 8 experienced slightly lesser T_{mrt} of 57.7°C. The latter is likely due to considerable extent of open spaces in LCZ 8, which in turn reflects less incoming shortwave solar radiation at noon time. However, during afternoon as the solar elevation angle decreases, more shade is provided by high-rise and mid-rise buildings in LCZ 1, 4, 5 and consequently exposure to high T_{mrt} is reduced.

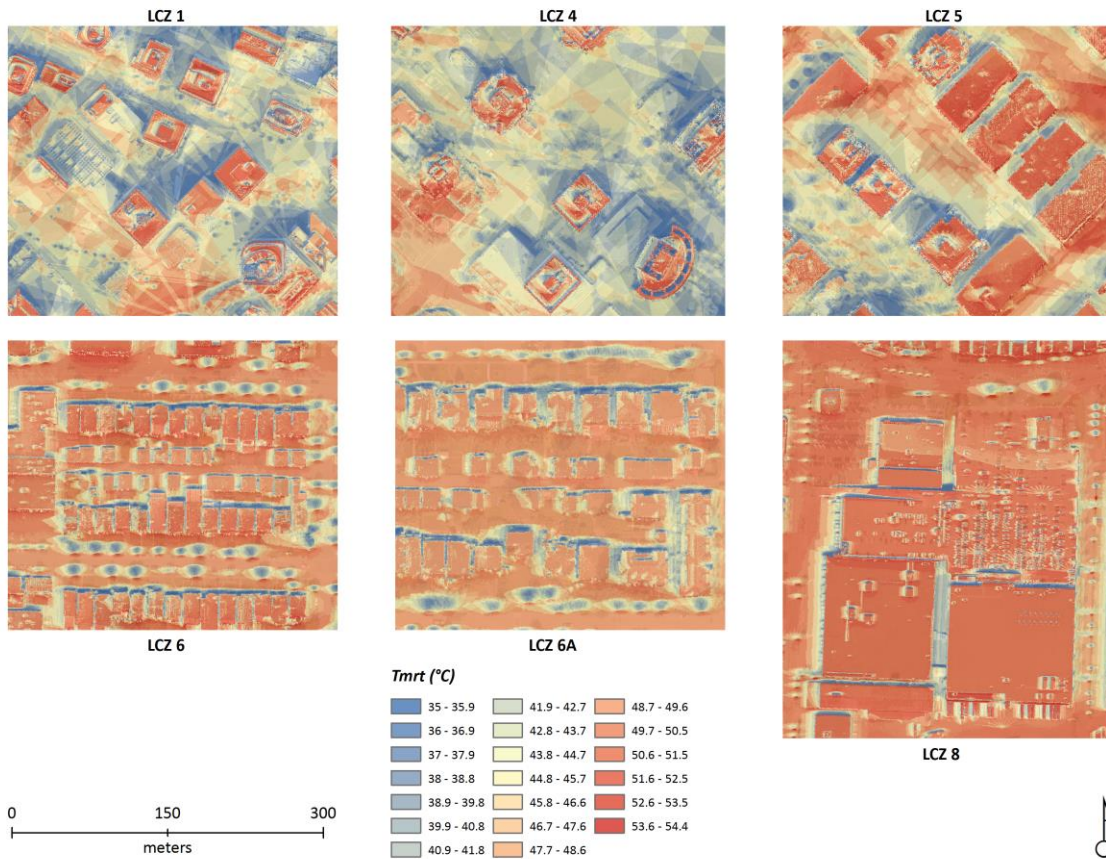


Figure 3-4: Variation of T_{mrt} values for six LCZs in Vancouver. The T_{mrt} values are averaged over the period from 9:00 – 18:00 for July 29, 2009.

3.4.3. Effects of increased street tree cover

All modeled T_{mrt} values were reduced after the addition of street trees representing a 1% increase of total plan area, for all LCZs (Table 3-2). The largest average T_{mrt} reduction was seen in the low-rise residential areas (LCZ 6 and 6A), where average T_{mrt} was reduced by 7.1°C for LCZ 6A and 6°C for LCZ 6, during the hottest part of the day. LCZs 1, 4 and 5 with relatively taller buildings and narrower streets are already well-shaded most of the day, so increasing street tree cover is less effective. It can be seen from the results that T_{mrt} is highly sensitive to street canopy change in LCZ 6 and 6A.

Figure 3-5 shows the spatial variability of T_{mrt} when 1% street tree cover is added to the simulations, and Figure 3-6 shows the change (Δ) in T_{mrt} after street tree addition relative to the case without added trees. The results show that the cooling effect of added street trees ranges

from 6-17°C in different LCZs, with the high end of that range being for a person standing right under a tree's canopy. The cooling potential of additional street trees varies among LCZs. For example, the effect of 1% increase of total plan area of tree cover is relatively greater in large low-rise areas (LCZ 8) compared to LCZ 1, 4 and 5 where shade is already casted by existing taller buildings.

Table 3-2: Spatial average of T_{mrt} before and after adding street trees. The data is shown for two time periods: all day from 9:00 – 18:00 and the hottest period of day from 11:00 – 17:00. ΔT_{mrt} measures the reduction in T_{mrt} due to 1% increase in street tree coverage.

Location	All day (9:00 – 18:00)			Hottest Period of Day (11:00 – 17:00)		
	T_{mrt}	Added Trees T_{mrt}	ΔT_{mrt}	T_{mrt}	Added Trees T_{mrt}	ΔT_{mrt}
LCZ 1	41.9	38.5	-3.4	43.6	40.3	-3.3
LCZ 4	43.5	39.9	-3.6	45.8	42.1	-3.7
LCZ 5	45.1	41.1	-4	46.7	43.1	-3.6
LCZ 6	47.5	41.7	-5.8	48.1	42.1	-6
LCZ 6A	47.2	40.9	-6.3	48.7	41.6	-7.1
LCZ 8	47.9	44.7	-3.2	49.7	45.1	-4.6

Several studies have investigated the effect of increased vegetation cover and green façades on summertime variation of T_{mrt} , albeit the focus of these studies was mainly on T_{mrt} for a single spot (Jänicke et al., 2015; Perini and Magliocco, 2014; Shashua-Bar et al., 2011; Taleghani et al., 2015). This study, however, expands the existing knowledge of the potential cooling of T_{mrt} due to urban greening by conducting T_{mrt} spatial analysis over six different LCZs, which represent typical urban environments in Vancouver, and in many cities across the world. In addition, this study simulated the spatial variation of T_{mrt} for an extreme hot weather day from 9:00 – 18:00 compared to that of a 1-hour temporal period in the previous studies. Although with different magnitude, reduction in T_{mrt} was modelled in all LCZs. This proves the potential cooling effect of urban greening through provision of shade, which will result in improved diurnal thermal exposure.

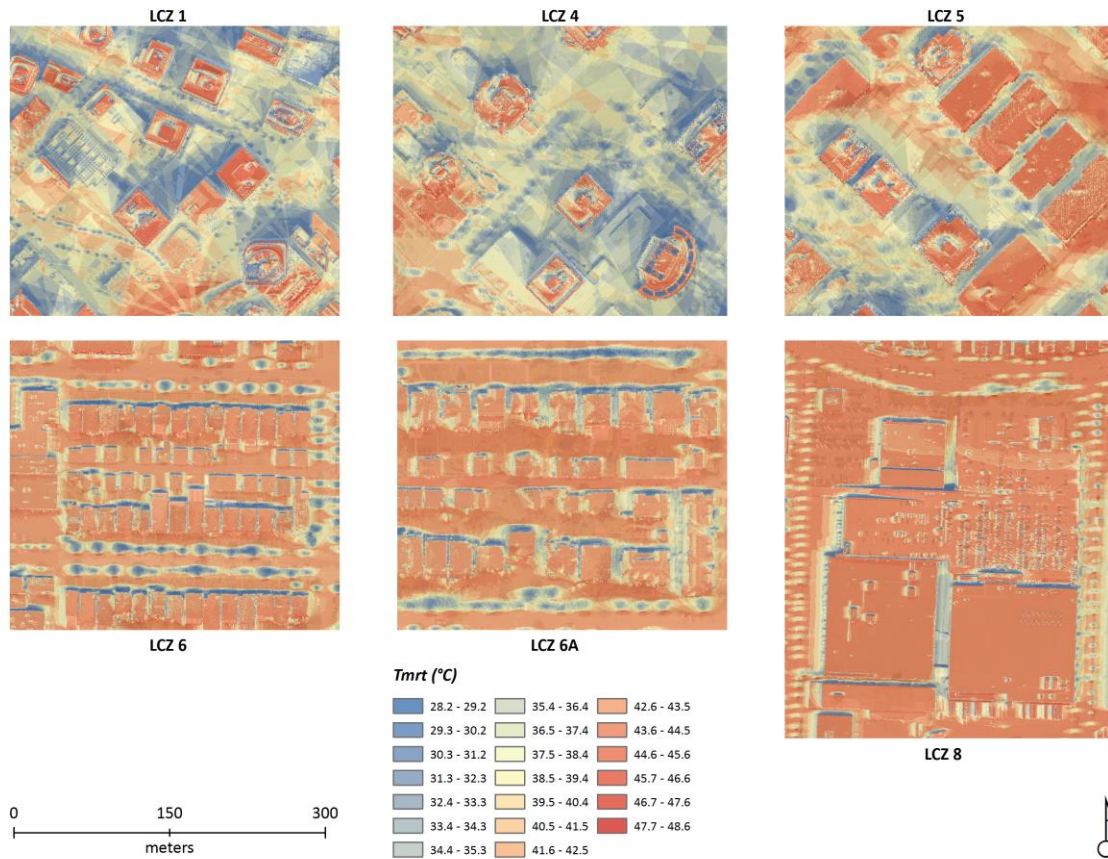


Figure 3-5: Variation of T_{mrt} values for 1% increase in street tree coverage in six LCZs in Vancouver. The T_{mrt} values are averaged over the period from 9:00 – 18:00 for July 29, 2009.

Although beyond the scope of this study, different driving factors of thermal exposure such as trees with matured crowns, tree clustering, reflective ground and wall surfaces should be taken into consideration if a comprehensive analysis is to be conducted in SOLWEIG. Currently, SOLWEIG has two known limitations: incapability of conducting nocturnal T_{mrt} analysis due to the structure of the model which relies on incoming solar radiation, and the exclusion of air flow and clothing insulation in T_{mrt} calculations. Yet, SOLWEIG has proven to perform well and successfully simulated the spatial variation of T_{mrt} in different urban settings with different climates (Chen et al., 2014; Jänicke et al., 2016, 2015, Lau et al., 2016, 2014; Lindberg et al., 2016; Thom et al., 2016; Thorsson et al., 2007). Models that more fully represent effects of urban trees on outdoor heat exposure are in development (Park et al. 2018).

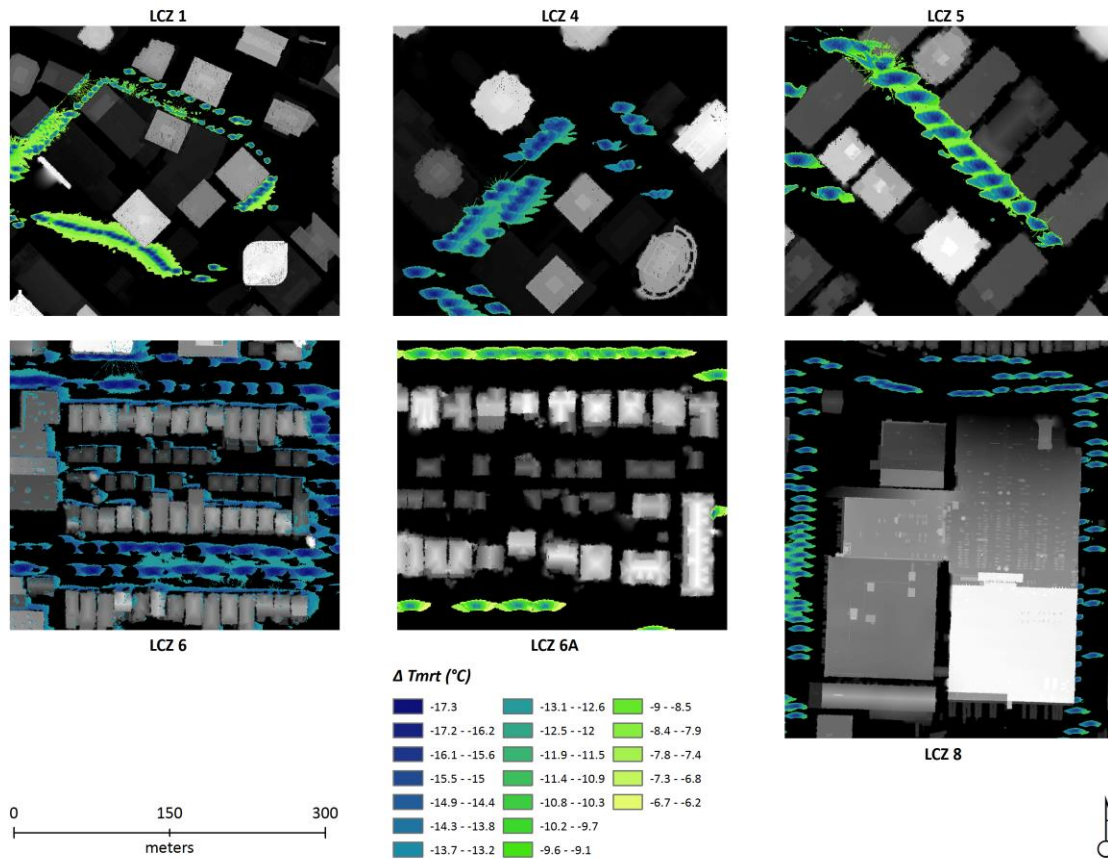


Figure 3-6: Change (ΔT_{mrt}) in the spatial distribution of T_{mrt} values before and after street tree inclusion scenarios in the simulation domain. The T_{mrt} values are averaged over the period from 9:00 – 18:00 for July 29, 2009 in six LCZs in Vancouver.

The novelty of this research lies in its unique approach to quantify T_{mrt} in mid-latitude neighborhoods categorized into LCZs in the coastal city of Vancouver. The LCZs approach also allows for a simpler comparison with similar neighborhoods in other mid-latitude coastal cities. Furthermore, the characterization of baseline T_{mrt} for common Vancouver LCZs during extreme hot summer days, prior to heat mitigation implementation or climate change, is unique to this study. The solution-oriented approach proposed here will provide tools and means to facilitate the integration of microscale climate knowledge into transferable urban design and planning practices for Vancouver.

3.5. Conclusion

This study investigated the spatial variability of T_{mrt} over six different LCZs in the large mid-latitude coastal city of Vancouver, Canada. The spatiotemporal changes in T_{mrt} were evaluated for the current land cover configurations, as well as for a simulated increase in street tree cover representing 1% of neighborhood area.

After successful evaluation of the SOLWEIG model against field observations, the results of this study identified LCZs in Vancouver where people outdoors are least or most exposed to heat. The compact high-rise neighborhood in downtown Vancouver (LCZ1) and large low-rise district (LCZ8) were the most and least thermally comfortable zones, respectively. Increasing street tree cover by 1% of plan area, as proposed in Vancouver's Urban Forestry Strategy, reduced neighborhood-average T_{mrt} and associated thermal exposure across all LCZs, with the greatest effect modeled to occur in low-rise residential areas (LCZ6 and 6A) where the additional trees provide shade that is otherwise relatively sparse.

While increasing the cover of trees on private lands will further reduce T_{mrt} , the addition of street trees to public sidewalks across the range of Vancouver's neighborhoods has direct cooling effects for pedestrians and will improve thermal exposure on hot summer days, including during periods of extreme hot weather.

The results of this study can inform city planners and decision makers on the specific spatiotemporal cooling effects expected from the addition of street trees, as a function of LCZ, and may help optimize such measures for creating a greener, cooler and healthier city. Also, it may potentially guide the city to prioritize the implementation of Vancouver's urban forestry strategy (Urban Forestry Strategy, City of Vancouver, 2014) into LCZs where higher T_{mrt} is observed currently and projected for future hot summer days.

3.6. Acknowledgments

The author acknowledges support from the Pacific Institute for Climate Solutions (PICS) fellowship program.

3.7. References

- Akbari, H., Pomerantz, M., Taha, H., 2001. "Cool surfaces and shade trees to reduce energy use and improve air quality in urban areas." *Solar Energy*. 70, 295-310.
- Akbari, H., Konopacki, S., 2005. "Calculating energy-saving potentials of heat-island reduction strategies." *Energy Policy*. 33, 721-756.
- Alexander, P.J., Fealy, R., Mills, G.M., 2016. "Simulating the impact of urban development pathways on the local climate: A scenario-based analysis in the greater Dublin region, Ireland." *Landscape and Urban Planning*. 152, 72-89.
- Aminipouri, M., Knudby, A., Ho, H.C., 2016. "Using multiple disparate data sources to map heat vulnerability: Vancouver case study." *Canadian Geographer*. 60, 356-368.
- Asaeda, T., Ca, V.T., Wake, A., 1996. "Heat storage of pavement and its effect on the lower atmosphere." *Atmospheric Environment*. 30, 413-427.
- Chen, L., Yu, B., Yang, F., Mayer, H., 2016. "Intra-urban differences of mean radiant temperature in different urban settings in Shanghai and implications for heat stress under heat waves: A GIS-based approach." *Energy and Buildings*. 130, 829-842.
- Chen, Y.-C., Lin, T.-P., Matzarakis, A., 2014. "Comparison of mean radiant temperature from field experiment and modelling: a case study in Freiburg, Germany." *Theoretical and Applied Climatology*. 118, 535-551.
- Erell, E., Pearlmuttere, D., Williamson, T., 2011. "Urban Microclimate: Designing the Spaces Between Buildings." *Earthscan*.
- Ho, H.C., Knudby, A., Xu, Y., Hodul, M., Aminipouri, M., 2016. "A comparison of urban heat islands mapped using skin temperature, air temperature, and apparent temperature (Humidex), for the greater Vancouver area." *Science of the Total Environment*. 544, 929-38.
- Holst, J., Mayer, H., 2011. "Impacts of Street Design Parameters on Human-Biometeorological Variables." *Meteorologische Zeitschrift*. 20 (5): 541-52.
- Höppe, P., 1992. "Ein neues Verfahren zur Bestimmung der mittleren Strahlungstemperatur im Freien." *Wetter und Leben*. 44.1-3, 147-151.
- Jänicke, B., Meier, F., Hoelscher, M.T., Scherer, D., 2015. "Evaluating the effects of facade greening on human bioclimate in a complex urban environment." *Advances in Meteorology*. 1-15.
- Jänicke, B., Meier, F., Lindberg, F., Schubert, S., Scherer, D., 2016. "Towards city-wide, building-resolving analysis of mean radiant temperature." *Urban Climate*. 15, 83-98.
- Konarska, J., Lindberg, F., Larsson, A., Thorsson, S., Holmer, B., 2014. "Transmissivity of solar

- radiation through crowns of single urban trees---application for outdoor thermal comfort modelling." *Theoretical and Applied Climatology*. 117, 363-376.
- Kosatsky, T., Henderson, S.B., Pollock, S.L., 2012. "Shifts in mortality during a hot weather event in Vancouver, British Columbia: rapid assessment with case-only analysis." *American Journal of Public Health*. 102, 2367-2371.
- Lau, K.K.-L., Lindberg, F., Rayner, D., Thorsson, S., 2014. "The effect of urban geometry on mean radiant temperature under future climate change: a study of three European cities." *International Journal of Biometeorology*. 59, 799-814.
- Lau, K.K.-L., Ren, C., Ho, J., Ng, E., 2016. "Numerical modelling of mean radiant temperature in high-density sub-tropical urban environment." *Energy and Buildings*. 114, 80-86.
- Lee, H., Mayer, H., 2018. "Maximum Extent of Human Heat Stress Reduction on Building Areas Due to Urban Greening." *Urban Forestry & Urban Greening*. 32, 154-67.
- Lee, H., Holst, J., and Mayer, H., 2013. "Modification of Human-Biometeorologically Significant Radiant Flux Densities by Shading as Local Method to Mitigate Heat Stress in Summer within Urban Street Canyons." *Advances in Meteorology*, 1-13.
- Lee, H., Mayer, H., Schindler, D., 2014. "Importance of 3-D Radiant Flux Densities for Outdoor Human Thermal Comfort on Clear-Sky Summer Days in Freiburg, Southwest Germany." *Meteorologische Zeitschrift*. 23 (3), 315-30.
- Lee, H., Mayer, H., Chen, L., 2016. "Contribution of trees and grasslands to the mitigation of human heat stress in a residential district of Freiburg, Southwest Germany." *Landscape and Urban Planning*. 148, 37-50.
- Lindberg, F., Grimmond, C.S.B., 2011a. "Nature of vegetation and building morphology characteristics across a city: Influence on shadow patterns and mean radiant temperatures in London." *Urban Ecosystems*. 14, 617-634.
- Lindberg, F., Grimmond, C.S.B., 2011b. "The influence of vegetation and building morphology on shadow patterns and mean radiant temperatures in urban areas: model development and evaluation." *Theoretical and Applied Climatology*. 105, 311-323.
- Lindberg, F., Holmer, B., Thorsson, S., 2008. "SOLWEIG 1.0 - Modelling spatial variations of 3D radiant fluxes and mean radiant temperature in complex urban settings." *Int. J. Biometeorol.* 52, 697-713.
- Lindberg, F., Onomura, S., Grimmond, C.S.B., 2016. "Influence of ground surface characteristics on the mean radiant temperature in urban areas." *International Journal of Biometeorology*. 60, 1439-1452.
- Lobaccaro, G., Acero, J.A., 2015. "Comparative analysis of green actions to improve outdoor thermal comfort inside typical urban street canyons." *Urban Climate*. 14, 251-267.
- Luber, G., Sanchez, C., Conklin, L., 2006. "Heat-related deaths in United States, 1999-2003."

- Morbidity and Mortality Weekly Report*. 29, 796-798.
- Martins, T.A.L., Adolphe, L., Bonhomme, M., Bonneaud, F., Faraut, S., Ginestet, S., Michel, C., Guyard, W., 2016. "Impact of Urban Cool Island measures on outdoor climate and pedestrian comfort: Simulations for a new district of Toulouse, France." *Sustainable Cities and Society*. 26, 9-26.
- Mayer, H. 1993. "Urban Bioclimatology." *Experientia*. 49 (11), 957-63.
- Mayer, H., Holst, J., Dostal, P., Imbery, F., Schindler, D., 2008. "Human Thermal Comfort in Summer within an Urban Street Canyon in Central Europe." *Meteorologische Zeitschrift*. 17 (3), 241-50.
- Middel, A., Häb, K., Brazel, A.J., Martin, C., Guhathakurta, S., 2014. "Impact of urban form and design on microclimate in Phoenix, Arizona." *Landscape and Urban Planning*. 122, 16-28.
- Middel, A., Chhetri, N., Quay, R., 2015. "Urban forestry and cool roofs: Assessment of heat mitigation strategies in Phoenix residential neighborhoods." *Urban Forestry and Urban Greening*. 14, 178-186.
- Middel, A., Selover, N., Hagen, B., Chhetri, N., 2016. "Impact of shade on outdoor thermal comfort---a seasonal field study in Tempe, Arizona." *International Journal of Biometeorology*. 1-13.
- Morakinyo, T.E., Lam, Y.F., 2016. "Simulation study on the impact of tree-configuration, planting pattern and wind condition on street-canyon's micro-climate and thermal comfort." *Building and Environment*. 103, 262-275.
- Oke, T.R., 1988. "The urban energy balance." *Progress in Physical Geography*. 12, 471-508.
- Open Data Catalogue, City of Vancouver, 2018. [Accessed online at <http://data.vancouver.ca/datacatalogue/index.htm> on July 9, 2018]
- Perini, K., Magliocco, A., 2014. "Effects of vegetation, urban density, building height, and atmospheric conditions on local temperatures and thermal comfort." *Urban Forestry and Urban Greening*. 13, 495-506.
- Reid, C.E., O'Neill, M.S., Gronlund, C.J., Brines, S.J., Brown, D.G., Diez-Roux, A. V, Schwartz, J., 2009. "Mapping community determinants of heat vulnerability." *Environmental Health Perspectives*. 117, 1730-1736.
- Salata, F., Golasi, I., Vollaro, A. de L., Vollaro, R. de L., 2015. "How high albedo and traditional buildings' materials and vegetation affect the quality of urban microclimate. A case study." *Energy and Buildings*. 99, 32-49.
- Santamouris, M., 2014. "Cooling the cities – A review of reflective and green roof mitigation technologies to fight heat island and improve comfort in urban environments." *Solar Energy*. 103, 682-703.

- Shashua-Bar, L., Pearlmutter, D., Erell, E., 2011. "The influence of trees and grass on outdoor thermal comfort in a hot-arid environment." *International Journal of Climatology*. 31, 1498-1506.
- Srivanit, M., Hokao, K., 2013. "Evaluating the cooling effects of greening for improving the outdoor thermal environment at an institutional campus in the summer." *Building and Environment*. 66, 158-172.
- Stewart, I.D., Oke, T.R., 2012. "Local Climate Zones for urban temperature studies." *Bulletin of the American Meteorological Society*. 93 (12), 1879-1900.
- Taleghani, M., Sailor, D.J., Tenpierik, M., van den Dobbela, A., 2014. "Thermal assessment of heat mitigation strategies: The case of Portland State University, Oregon, USA." *Building and Environment*. 73, 138-150.
- Taleghani, M., Kleerekoper, L., Tenpierik, M., van den Dobbela, A., 2015. "Outdoor thermal comfort within five different urban forms in the Netherlands." *Building and Environment*. 83, 65-78.
- Thom, J.K., Coutts, A.M., Broadbent, A.M., Tapper, N.J., 2016. "The influence of increasing tree cover on mean radiant temperature across a mixed development suburb in Adelaide, Australia." *Urban Forestry and Urban Greening*. 20, 233-242.
- Thorsson, S., Lindberg, F., Eliasson, I., Holmer, B., 2007. "Different methods for estimating the mean radiant temperature in an outdoor urban setting." *International Journal of Climatology*. 27, 1983-1993.
- Thorsson, S., Lindberg, F., Björklund, J., Holmer, B., Rayner, D., 2011. "Potential changes in outdoor thermal comfort conditions in Gothenburg, Sweden due to climate change: the influence of urban geometry." *International Journal of Climatology*. 31, 324-335.
- Urban Forestry Strategy, City of Vancouver, 2014. [Accessed online at <https://vancouver.ca/files/cov/Urban-Forest-Strategy-Draft.pdf> on July 9, 2018]
- VDI. 1994. Environmental Meteorology - Interactions between Atmosphere and Surfaces - Calculation of Short-Wave and Long-Wave Radiation. The Association of German Engineers, VDI 3789, Part 2.
- World Cities Report, United Nations, 2016. [Accessed online at <http://wcr.unhabitat.org/main-report/> on July 9, 2018]
- Zölch, T., Maderspacher, J., Wamsler, C., Pauleit, S., 2016. "Using green infrastructure for urban climate-proofing: An evaluation of heat mitigation measures at the micro-scale." *Urban Forestry and Urban Greening*. 20, 305-316.

Chapter 4. Urban tree planting and outdoor thermal comfort in the face of global warming: The case of Vancouver's local climate zones

This chapter has been published in the Building and Environment journal.

Citation details: Aminipouri, M., Rayner, D., Lindberg, F., Thorsson, S., Knudby, A., Zickfeld, K., Middel, A., and Krayenhoff, E.S., 2019. "Urban tree planting and outdoor thermal comfort in the face of global warming: The case of Vancouver's local climate zones." Building and Environment 158, 226-236.

Contribution statement: First author outlined the research idea with support from Dr. Kirsten Zickfeld, Dr. David Rayner, Prof. Sofia Thorsson and Dr. Fredrik Lindberg, designed the simulations with support from Dr. David Rayner and Dr. Fredrik Lindberg, performed the analysis and wrote the manuscript. All co-authors provided feedback and edited the manuscript.

4.1. Abstract

Spatiotemporal variation of mean radiant temperature (T_{mrt}), a major driver of outdoor human thermal comfort, is affected by local microclimate conditions, including exposure to solar and longwave radiation, shading, wind and air temperature. In this study, the SOLar and LongWave Environmental Irradiance Geometry (SOLWEIG) model was used to simulate how changes in minimum and maximum air temperature and solar radiation under Representative Concentration Pathways (RCP) 4.5 and 8.5 climate projections would change T_{mrt} in Vancouver over the 2070-2100 period. With micrometeorological variables representing a changed climate, days with extreme radiant heat load were predicted to increase three- to five-fold under RCP 4.5 and 8.5, respectively. SOLWEIG was also used to quantify the potential of maximum feasible street tree cover to reduce T_{mrt} for the hottest day on record for Vancouver (July 29, 2009), and an end-of-century hot day under the two future climate scenarios. SOLWEIG simulations with maximum feasible street tree cover under RCP 4.5 demonstrated an average reduction of 1.3°C

in T_{mrt} , compared to the contemporary observation day with current street trees. However, averaged T_{mrt} increased by 1.9°C under the RCP 8.5 scenario even with maximum feasible street tree cover. We conclude that adding street trees has the potential to reduce T_{mrt} under the RCP 4.5 scenario, however the measure is insufficient to decrease or maintain T_{mrt} under the RCP 8.5 scenario. From an urban planning perspective, complimentary heat mitigation measures may be required if outdoor thermal comfort is to be maintained in Vancouver during the century.

Keywords: Mean radiant temperature, SOLWEIG, Local climate zones, Extreme radiant thermal exposure, Heat mitigation, Street trees.

4.2. Introduction

Rapid urbanization is often associated with extensive land cover changes, increased air pollution, anthropogenic heating, and reduced evaporation from limited urban greenery (Oliveira et al. 2011). These can alter surface and air temperature, shading, near-surface humidity, wind patterns and ultimately human thermal comfort (Argüeso et al. 2015; Shashua-Bar et al. 2011). Various thermal comfort indices have been used by researchers to evaluate heat vulnerability and thermal exposure. Heat vulnerability is often assessed by predictors such as land surface temperature (T_s), air temperature (T_a) and humidex (Aminipouri et al. 2016; Ho et al. 2015), while thermal comfort is mainly evaluated by physiologically equivalent temperature (PET) (Yang and Lin 2016; Ali-Toudert and Mayer 2007; Lee et al. 2016; Höppe 1999), universal thermal climate index (UTCI) (Jendritzky et al. 2012; Park et al. 2014) and mean radiant temperature (T_{mrt}) (Yang and Lin 2016; Lau et al. 2014; Chen et al. 2016; Thorsson et al. 2014, 2017; Middel et al. 2016). The latter, T_{mrt} , is a synthetic biometeorological driver of human thermal comfort and is defined as the surface temperature of a reference human in radiative equilibrium with their environment (Thorsson et al. 2007). T_{mrt} has been recently used for thermal exposure studies (Yang and Lin 2016; Lindberg and Grimmond 2011a; Park et al. 2016) and its magnitude and spatial distribution is found to be influenced by the location and spatial pattern of trees (Thom et al. 2016; Kong et al. 2017; Ng et al. 2015).

The presence of urban greenery and street trees in urban areas has been shown to moderate radiant heat load and thermal discomfort by lowering T_{mrt} (Kong et al. 2017; Thom et al. 2016). For example, in the vicinity of green walls, T_{mrt} was reduced by 2°C in a study

conducted in Berlin, Germany (Jänicke et al. 2015). Also, in close proximity to street trees, T_{mrt} decreased by 7°C in a case study in Freiburg, Germany (Lee et al. 2016) and 10°C in a research case in Bilbao, Spain (Lobaccaro and Acero 2015). In recent years, considerable attention has been given to heat mitigation measures and their impacts on urban microclimate under the current climate (Kong et al. 2017; Chen et al. 2014; Lau et al. 2016; Thom et al. 2016; Zölch et al. 2016). The influence of projected future warming on human thermal comfort and its contribution to T_{mrt} variations across different neighborhoods classified into local climate zones (LCZs) (Stewart and Oke 2012) has yet to be examined.

The LCZ approach introduced by Stewart (2011) classifies landscape types into ten urban classes, seven non-urban classes, and a range of mixed classes, based on their impact on the surface air temperature. LCZs are classified based on their surface properties (i.e. albedo, height-to-width ratio, sky view factor, tree and building height), which are measurable and independent of time or space. Such class definition makes the LCZ methodology a universally comparable approach for urban microclimatology studies, and facilitates knowledge transfer between urban climatologists, planners and practitioners (Alexander et al. 2016).

Studies focused on T_{mrt} in a projected future climate for different LCZs are hence valuable. To mitigate negative effects of extreme radiant thermal exposure induced by projected climate, it is crucial to identify and predict micrometeorological conditions which generate heat vulnerability and extreme heat stress. Projected intense heat waves, characterized by high T_a , exposure to solar and longwave radiation, and low wind speed, will build undesirable heat load on humans (Mayer et al. 2008; Thorsson et al. 2017). Heat mitigation actions also require high accuracy detection of spaces prone to heat within different LCZs.

Global or regional climate models provide tools to evaluate climate change impacts on T_{mrt} . However, the limited spatial resolution of global climate models (GCMs) (150-300 km) and regional climate models (RCMs) (25-50 km) (Lau et al. 2014) makes it very difficult to estimate the effects of climate change on cities at the neighborhood scale. To overcome this limitation, several numerical and statistical downscaling techniques have been developed to generate multi-variable time-series climate data at finer spatial resolution on daily or monthly time scales (Benestad 2011). Although applying these types of downscaling techniques will reduce bias in

the simulated data, these data are still not adequately close to observed data (Lindberg et al. 2016) and therefore cannot be used as an input for further climate impact modeling. Thus, the simulated data, even from RCMs, must be rescaled to accurately estimate the effect of projected changes to micrometeorological variables on changes in the heat comfort indices. For example, Koffi and Koffi (2008) rescaled outputs from a European RCM from observation-based to percentile-based threshold values. Rivington et al. (2008) used a downscaling method to recalibrate RCM estimates of precipitation, daily maximum and minimum air temperature, and solar radiation to improve the match between simulated and observed climate data. Studying urban microclimates in a climate change perspective requires future projections at a finer spatiotemporal resolution. In this regard, Rayner et al. (2015) developed a statistical downscaling method that combines hourly observations of meteorological parameters with change factors from daily climate model outputs to ultimately generate hourly climate scenario time series.

More intense, frequent, and long-lasting heatwaves are anticipated under climate change scenarios. This increase will have adverse effects on human thermal exposure. Therefore, the overall objective of this research is to quantify the ability of a proposed heat mitigation strategy (increased street tree cover to maximum feasible number) to reduce or maintain current T_{mrt} under projected climate scenarios for selected LCZs in Vancouver. The specific research questions under investigation are as follows:

- Compared to the present day, which changes in the spatiotemporal distribution of T_{mrt} would occur in selected LCZs under future climate scenarios, given no change in street tree cover?
- Under future climate scenarios, what changes in spatiotemporal variations of T_{mrt} are projected if the maximum feasible number of trees are planted in selected LCZs in Vancouver?

Using the solar and longwave environmental irradiance geometry (SOLWEIG) model (Lindberg et al. 2008), the T_{mrt} experienced along a representative pedestrian route was simulated for selected LCZs for July 29, 2009, the hottest day ever recorded in Vancouver, as well as for an end-of-century hot day. Simulations were performed with both present-day vegetation and a maximum-feasible-trees scenario. To simulate conditions for an end-of-century hot day, the input meteorological data was modified using the method of Rayner et al. (2015)

based on outputs from the Canadian Earth System Model (CanESM2) model downscaled with the Canadian Regional Climate Model (CanRCM4) (Scinocca et al. 2016), under Representative Concentration Pathways (RCP) 4.5 and 8.5.

This study provides new knowledge to city planners and decision makers for supporting their efforts in urban development programs at the neighborhood and street scales to minimize radiant heat load and improve outdoor thermal comfort.

4.3. Materials and methods

4.3.1. Study area

The city of Vancouver is located at 49.2°N latitude in the southwestern corner of the province of British Columbia, Canada. Vancouver is surrounded by mountains to the north, by the Pacific Ocean to the west, and a relatively flat interior to the east, a topographically complex urban form that generates diverse microclimates (Runnalls and Oke 2000; Voogt and Oke 1997).

Selected LCZs that represent typical Vancouver neighborhoods and for which digital surface models of buildings and trees as well as micrometeorological data were available, include: compact high-rise (LCZ 1), open high-rise (LCZ 4), open mid-rise (LCZ 5), open low-rise (LCZ 6), open low-rise with dense-trees (LCZ 6A), and large low-rise (LCZ 8). The studied area of each LCZ covers approximately 300*300 m, laid out on east-west, north-south or at approximately 45° to the cardinal directions of street networks (Figure 4-1). The aerial view and sky view photographs of selected LCZs and their physical properties are shown in Figure 4-2.

4.3.2. Meteorological data

Sub-hourly (i.e. 30-minute temporal resolution) meteorological data, including air temperature (T_a , °C), relative humidity (RH, %) and global solar radiation (Wm^{-2}), were obtained from an urban climate tower station operated by the University of British Columbia (UBC) in the Sunset residential neighborhood (Figure 4-1). Diffuse and direct radiation were estimated from the measured global radiation component, for both observed and future climate scenarios, using the method of Reindl et al. (1990). The dataset covers 10 years of measurements from

2008-2017 for which Ta and RH were measured at 1.2 m height and global solar radiation was measured at 26 m height.



Figure 4-1: The location of selected LCZs and climate tower station in Vancouver, British Columbia, Canada.

4.3.3. Climate change scenarios

Spatiotemporal variations of T_{mrt} for future years (2070-2100) were simulated by using a change-factor algorithm to modify the observed meteorological data (2008-2017) to reflect climate changes simulated by an Earth System Model/Regional Climate Model under RCP 4.5 and 8.5 climate scenarios. The RCP 4.5 scenario considers the total radiative forcing to be stabilized at 4.5 Wm^{-2} by 2100 (Moss et al. 2010), while the RCP 8.5 scenario represents an

intensive fossil-fuel use scenario resulting in comparatively high radiative forcing by 2100 (8.5 Wm⁻²) (Riahi et al. 2008).

Changes in daily climate between the period 1998-2027 (i.e. observations +/- 10 years) and 2070-2100 were calculated based on the outputs from the Canadian Regional Climate Model 4th generation (CanRCM4) (Scinocca et al. 2016) for which the parent model was the second-generation Canadian Earth System Model (CanESM2). CanESM2 is an Earth System Model (ESM) developed by the Canadian Centre for Climate Modelling and Analysis of Environment and Climate Change Canada as their contribution to the Intergovernmental Panel on Climate Change (IPCC) fifth assessment report (AR5) (Arora et al. 2011). Outputs from RCMs are preferred for urban planning purposes as they simulate climate change patterns at a finer scale than global models (Thorsson et al. 2017).

The differences in daily climate between 1998-2027 and 2070-2100 were used to calculate sub-daily change factors using an algorithm based on Rayner et al. (2015), and these differences were then applied to the observed meteorological data (2008-2017) to generate sub-hourly future micrometeorological scenarios. To create sub-hourly T_a scenarios, change factors for daily minimum and maximum T_a were calculated from the ranked changes in the CanRCM4 minimum and maximum T_a outputs for both RCP 4.5 and 8.5 scenarios. Then, using linear interpolation, change factors for every sub-hourly T_a value for each day in the observation period were determined. That is, the change in temperature between the hottest day in the modelled period 1998-2027 and the hottest day in the 2070-2100 period was the change factor applied to the hottest day in the historical record, and likewise for all other days based on their percentile ranking.

Change factors for sub-hourly global radiation for each day in the observation period were calculated based on the differences in the ranked daily global radiation in the CanRCM4 outputs. The fractional change in daily global radiation for each day was applied to all sub-hourly global radiation values for the day. Sub-hourly diffuse and direct solar radiation values were estimated from the global radiation component, both for the observations and all climate scenarios using a method by Reindl et al. (1990).

Unchanged observed sub-hourly RH values were used in the future climate simulations. It has been shown in earlier studies that estimation of T_{mrt} in SOLWEIG is not influenced by the

changes in RH whereas it is most sensitive to shortwave solar radiation and T_a (Onomura et al. 2015; Lindberg et al. 2016; Zölch et al. 2016).

LCZs	Site Photographs		Site properties ¹	LCZ schematics ²
	Aerial view	Sky view		
LCZ 1			SVF 0.2 % built-up >95 Z_H 75-100	
LCZ 4			SVF 0.5 % built-up 80 Z_H 50-75	
LCZ 5			SVF 0.55 % built-up 85 Z_H 15-30	
LCZ 6			SVF 0.75 % built-up 45-55 Z_H 5-10	
LCZ 6A			SVF 0.7 % built-up 40-50 Z_H 7-15	
LCZ 8			SVF 0.77 % built-up >95 Z_H 5	

Figure 4-2: Aerial view and sky view of selected LCZs in Vancouver. The study areas are: LCZ 1 compact high-rise; LCZ 4 open high-rise; LCZ 5 open-mid-rise; LCZ 6 open low-rise; LCZ 6A open low-rise with dense trees; and LCZ 8 large low-rise.

¹ Sky View Factor (SVF); % built-up= the sum of ground-level impervious and building surfaces fractions; Z_H =geometric average of building or plant-canopy heights (m). ² LCZ schematics are adopted from Stewart (2011).

4.3.4. Projected changes in meteorological variables and assessment of extreme radiant thermal exposure

SOLWEIG 1D (Lindberg et al. 2014) was used to analyze the temporal development of T_a , global radiation and T_{mrt} for the observation period and future RCP 4.5 and 8.5 scenarios. SOLWEIG 1D calculates the variations of T_a , global radiation and T_{mrt} for a generic location assumed to be sunlit during the day with a fixed SVF value of 0.6. Other meteorological, environmental, and human exposure parameters similar to the ones used in the full version of SOLWEIG were applied here. To significantly reduce computational time, SOLWEIG 1D is used for the temporal assessment of micrometeorological variables over present- and future-day scenarios.

Here, $T_{mrt} \geq 65^\circ\text{C}$ is used to represent extreme radiant thermal exposure (i.e. extreme heat stress) (Holst and Mayer 2010; Lee et al. 2013; Pantavou et al. 2018; Park et al. 2014; Thorsson et al. 2017). It should be noted that the definition of extreme radiant heat exposure and how thermal conditions are perceived might differ in different cities due to their local adaptation and acclimatization to extreme heat (Baccini et al. 2008). Nevertheless, a baseline threshold values of T_{mrt} is needed to be able to make comparison across cities or LCZs.

The average number of days per year, average number of consecutive days per year (two or more days), average number of weeks (seven consecutive days) per year, and average number of consecutive hours per year for which $T_{mrt} \geq 65^\circ\text{C}$ were calculated for the observation period as well as for both RCP 4.5 and 8.5 scenarios.

4.3.5. Simulations of T_{mrt} in SOLWEIG

Spatiotemporal variations of T_{mrt} for a single extreme hot summer day for the observation period and RCP 4.5 and 8.5 scenarios across all LCZ case studies were simulated using the SOLWEIG model (Lindberg et al. 2008; Lindberg and Grimmond 2011b). SOLWEIG requires few meteorological variables (i.e. T_a , RH, global, diffuse and direct solar radiation), geographical location of the study sites as well as digital surface models of buildings and trees, a digital elevation model (DEM) and sky view factor (SVF). For each LCZ, digital surface models of buildings and trees, DEM, and SVF were created using the publicly available 0.3 m-resolution

light detection and ranging (LiDAR) data obtained from City of Vancouver's open data catalogue ("Open Data Catalogue, City of Vancouver," 2019). SOLWEIG also needs environmental and human exposure setup configurations. The default environmental parameters were used: albedo of walls (0.2), albedo of ground surfaces (0.15), emissivity of walls (0.9) and emissivity of ground surfaces (0.95), according to Steyn and Oke (1980) and Oke and Cleugh (1987). T_{mrt} is then calculated for a standing person with standard values of absorption coefficient of 0.7 and 0.95 for shortwave and longwave radiations, respectively.

The SOLWEIG model was evaluated for Vancouver LCZs in a prior study (Aminipouri et al. 2019). Good agreement was shown between measured and modelled T_{mrt} across all six LCZs. The model explains 85% to 94% of T_{mrt} variations for different LCZs with an overall mean absolute error (MAE) of 3.7°C and root mean square error (RMSE) of 4.4°C. For a detailed description of the SOLWEIG validation process across all six LCZs in Vancouver, please refer to Aminipouri et al. (2019).

The simulations were conducted under two different street tree cover settings: a) current street tree cover and b) maximum feasible number of street trees. The maximum feasible number of street trees was achieved by following the street tree planting standards used by the City of Vancouver (City of Vancouver 2011). The standard states that new medium size trees need to be planted at least 6 meters apart. The influence of the maximum feasible number of street trees on variations of T_{mrt} was then evaluated by adding street trees to the plan area of each site and re-running the model. Trees were added considering the following criteria:

- Since the space between street trees is already very limited in Vancouver, a careful planting strategy was followed to make sure new trees are planted 6 meters away from existing trees.
- Only deciduous trees typical of Vancouver's existing street trees were added, with 4m crown diameter, 2.6m trunk height and 7m tree height.
- Regardless of street orientation, trees were added to all publicly accessible sidewalks and lawns adjacent to sidewalks to ensure spatial variations of T_{mrt} are captured thoroughly.

- Due to limited available data, minimum distances trees should be planted from street infrastructure (e.g. traffic signs and utility lines, fire hydrants, benches, etc.) were not considered in simulations.

Adding the maximum feasible number of street trees resulted in the additions of 155 trees in LCZ 1, 110 trees in LCZ 4, 50 trees in LCZ 5, 55 trees in LCZ 6, 55 trees in LCZ 6A and 120 trees in LCZ 8. These additions translate into approximately a 1.2% plan area increase in street tree cover in the six LCZs. The number of added street trees differs primarily because the current tree density varies among LCZs.

T_{mrt} values were then obtained using a point traverse extraction method. In this method a hypothetical pedestrian completed a closed traverse (i.e. originating from a point and returning to the same point) around each LCZ, and T_{mrt} values were extracted for random positions along the traverse. Using this approach, approximately 200-300 randomly distributed points were obtained for each LCZ, which captured a comprehensive pedestrian-based representation of T_{mrt} variations.

4.4. Results and discussion

4.4.1. Projected changes in micrometeorological variables

The observed micrometeorological variables (T_a , global radiation and T_{mrt}) were compared to future climate scenarios across the annual cycle and are presented in the following sections. However, summer months are the focus of the discussion (i.e. June, July and August) when extreme heat events are common.

4.4.1.1. Air temperature

The observed monthly-averaged daily maximum and minimum T_a and the difference between observed and future RCP 4.5 and 8.5 scenarios are presented in Figure 4-3.

The downscaled projections show an increase in maximum and minimum T_a values for both RCP scenarios in Vancouver, as has also been shown for other Canadian cities (Benmarhnia et al. 2014; Wang et al. 2015) and previously for the Vancouver area (Metro Vancouver 2016).

However, the magnitude of the maximum and minimum T_a change differed within RCP scenarios and across seasons. For example, the monthly-average maximum and minimum T_a , for summer season, changed by the same amount of 2.2°C in RCP 4.5 scenario, whereas in the fall season, the monthly-average minimum T_a (i.e. late night-early morning) increased 1.1°C more than monthly-average maximum T_a (i.e. hottest period of day). During extreme heat events, increase in minimum air temperature (i.e. nighttime temperature) increases the prevalence of elevations in body core temperature and consequently heat stress symptoms over a prolonged period and can cause various degrees of thermoregulatory failure and hence exacerbates heat-health mortality especially for the elderly population (Benmarhnia et al. 2014; Besancenot 2002; Goodman 2004; Laaidi et al. 2012).

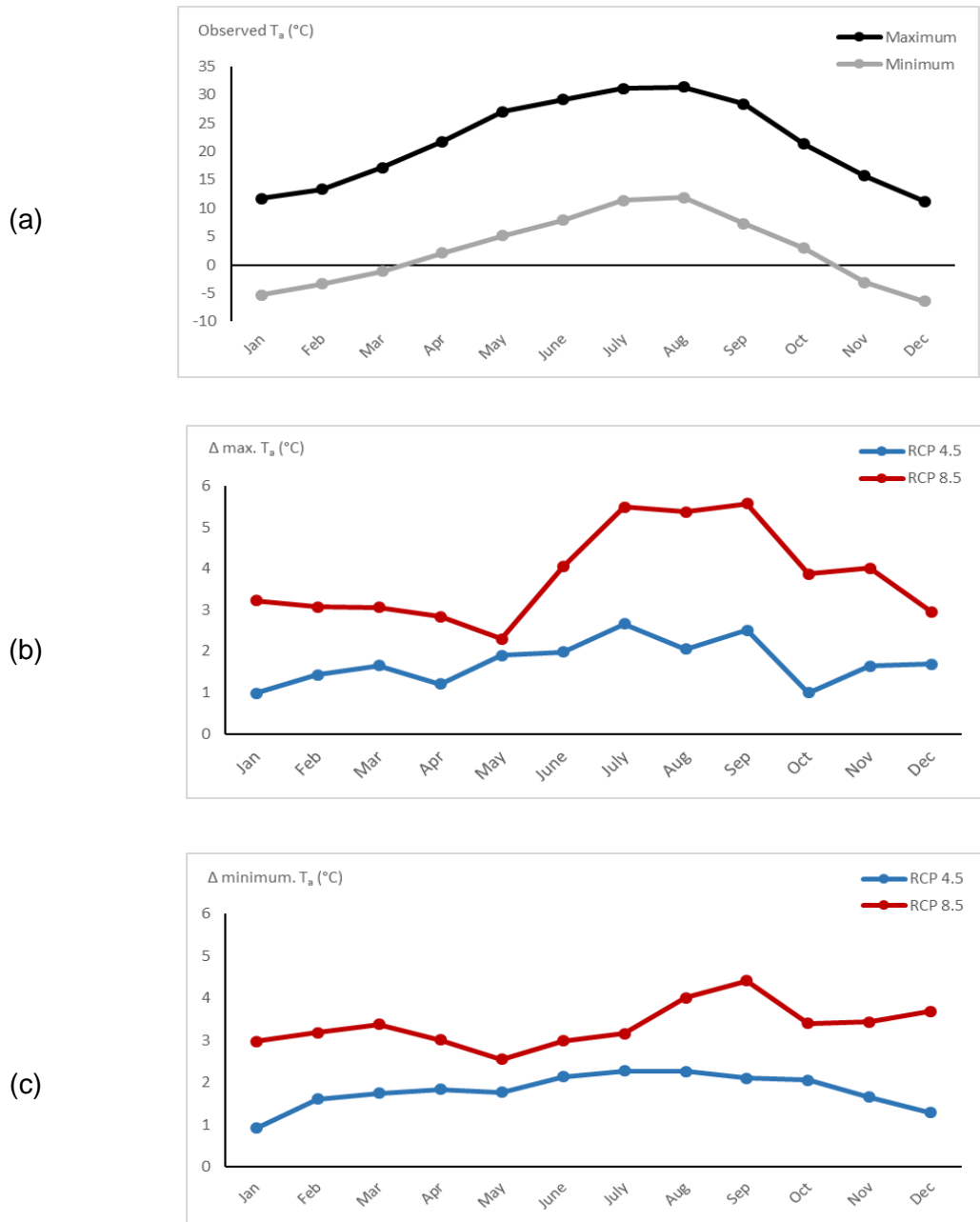


Figure 4-3: (a) Observed monthly-averaged daily maximum and minimum T_a across the annual cycle; (b) difference between observed and future RCP 4.5 and 8.5 scenarios in monthly-averaged daily maximum T_a across the annual cycle; (c) difference between observed and future RCP 4.5 and 8.5 scenarios in monthly-averaged daily minimum T_a across the annual cycle. Observation record is from 2008-2017 and climate scenarios are from 2070-2100.

Note that in RCP 8.5, compared to observation period, the biggest changes in monthly-average maximum (+5.6°C) and minimum (+4.4°C) T_a occur from the middle of the summer to the early fall, which is already the hottest part of the year.

4.4.1.2. Global shortwave radiation

Figure 4-4 illustrates the monthly-averaged daily global shortwave radiation for the observation period as well as for the future climate scenarios, RCP 4.5 and 8.5, relative to the observation period. As expected, global shortwave radiation peak around the summer season. Under the RCP 4.5 scenario and among summer months, the only decrease in global shortwave radiation occurs in June (-2 Wm^{-2}), whereas under RCP 8.5 both June and July experienced reduction in global shortwave radiation (-1.5 - -2 Wm^{-2}). The relatively small reductions in global shortwave radiation in the summer months in these cases can be attributed to a projected increase in cloudiness in the Vancouver area. A similar behaviour of monthly-averaged daily global radiation changes over future periods was observed in Frankfurt (50°N), Germany, in a study conducted by (Thorsson et al. 2017) in which a -3 Wm^{-2} reduction in summer-monthly-averaged global shortwave radiation was indicated.

4.4.1.3. Mean radiant temperature and extreme radiant thermal exposure

Figure 4-5 shows the monthly-averaged daily maximum and minimum T_{mrt} and the projected changes in future climate scenarios. As can be seen from Figure 4-5(a), the monthly-averaged daily maximum T_{mrt} is consistently around 66°C across the summer months. The projected future changes of maximum and minimum T_{mrt} (Figure 4-5(b) and 4-5(c)) followed a similar pattern to maximum and minimum T_a , with a steady increase in T_{mrt} in both RCP 4.5 and 8.5 scenarios during the summer. T_{mrt} also increased in winter months under both RCP scenarios, as a result of increases in T_a .

Extreme radiant thermal exposure is assessed for the observation period and both climate scenarios (Table 4-1). The average number of days per year with $T_{mrt} \geq 65^\circ\text{C}$ quintupled from 8 days in the observation period to 40 days in RCP 8.5 scenario. The average number of consecutive days per year (two or more days) with $T_{mrt} \geq 65^\circ\text{C}$ also grew fivefold from 6 days in the observation period to 33 days in RCP 8.5 scenario. The average number of weeks (seven

consecutive days) per year with $T_{mrt} \geq 65^\circ\text{C}$ increased from 0.1 week in the observation period (i.e. once every 10 years) to 2.1 weeks per year in RCP 8.5 (Table 4-1).

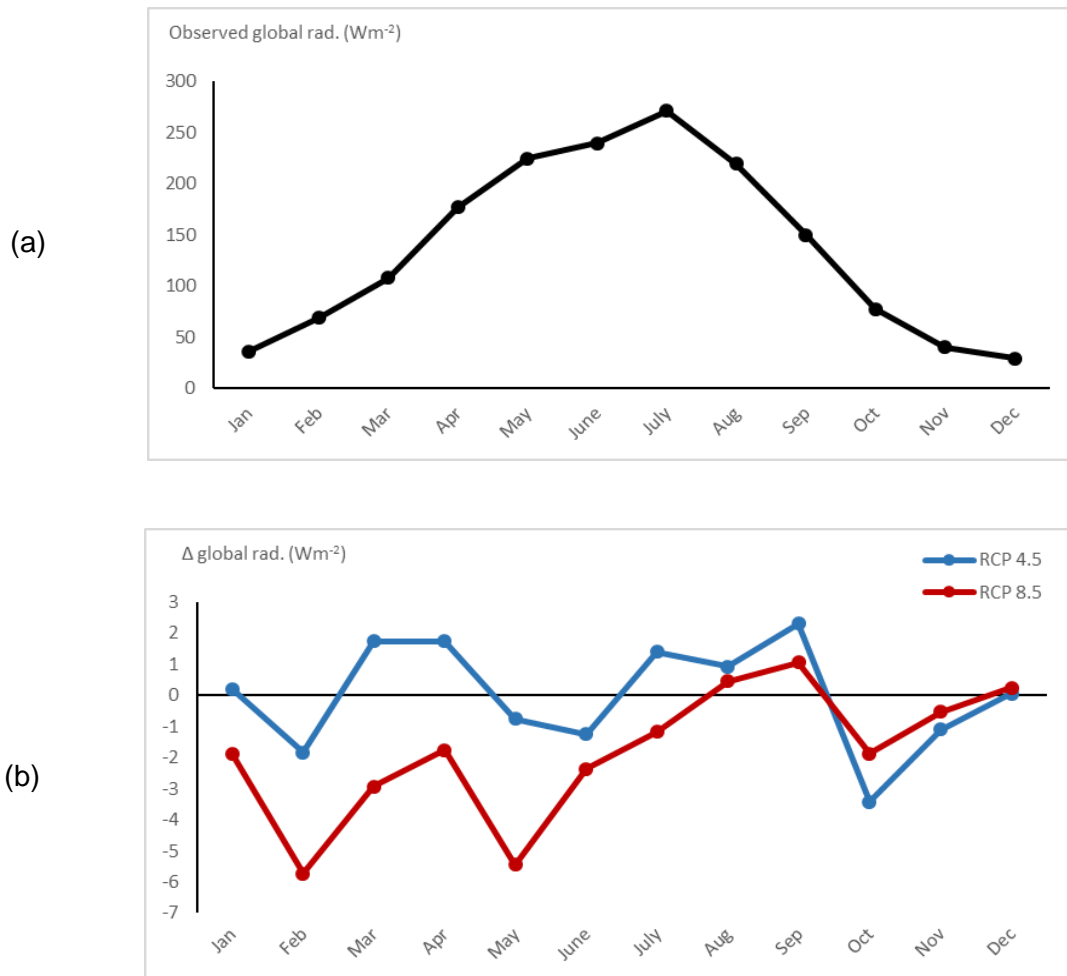


Figure 4-4: (a) observed monthly-averaged daily global shortwave radiation; (b) difference between RCP 4.5 and 8.5 scenarios and observation period in monthly-averaged daily global shortwave radiation. Observation record is from 2008-2017 and climate scenarios are from 2070-2100.

The large differences in the average number of extreme hot days (i.e. $T_{mrt} \geq 65^\circ\text{C}$) between the observation period and RCP 4.5 and 8.5 can be explained by two factors. Firstly, spatiotemporal variations of T_{mrt} can be very large even with a small change in T_a and global radiation (Mayer et al. 2008; Lau et al. 2014). According to Figure 4-4-b, unlike the June of RCP 4.5 and 8.5 and the July of RCP 8.5 where negative changes in global shortwave radiation were shown, other summer months were projected to experience greater global radiation than that

of the observation period. On the other hand, summer-averaged daily maximum T_a increased by 2.3°C and 5.5°C for RCP 4.5 and 8.5 respectively. An overall increase in T_a combined with the effects of global shortwave radiation triggered an increase in T_{mrt} . Secondly, there were many consecutive days and hours close to the $T_{mrt} \geq 65^\circ\text{C}$ threshold in the observation period. Therefore, a small increase in T_{mrt} led to a comparatively large increase in the number of days with $T_{mrt} \geq 65^\circ\text{C}$ in the future, an effect that was also noticed by (Thorsson et al. 2017) in Frankfurt, Germany, which is located at a similar latitude to Vancouver. The increasing number of consecutive hours, days, and weeks when $T_{mrt} \geq 65^\circ\text{C}$ suggests that extreme radiant thermal exposure will worsen under both RCP 4.5 and 8.5 climate scenarios. This will exacerbate heat-health vulnerability especially in Vancouver's neighborhoods where at the same time vulnerability to heat is increasing (Aminipouri et al. 2016; Ho et al. 2018).

4.4.2. Spatial variations of T_{mrt} under RCP 4.5 and 8.5

An ensemble of 36 simulations was run in SOLWEIG, consisting of all combinations of three different climate scenarios (observation, RCP 4.5 and 8.5) and two street tree planting options (existing tree coverage, and maximum feasible number of street trees) for all six LCZs. For each of the 36 simulations, spatially averaged T_{mrt} values were extracted for publicly accessible sidewalks over the hottest period of the day, 11:00-17:00 (Table 4-2).

Variations in T_{mrt} across all six LCZs were modelled for 11:00-17:00, July 29, 2009 and compared to the same time of day for the hottest day in the 2070-2100 period, under both RCP 4.5 and 8.5 climate scenarios. On the observation day, average T_{mrt} ranged between 51.1°C and 61.1°C, making LCZ 1 (compact high-rise) the most and LCZ 8 (large low-rise) the least thermally comfortable LCZs in Vancouver. Under the RCP 4.5 and 8.5 scenarios, T_{mrt} increased on average by 1.75°C and 4.8°C respectively across LCZs.

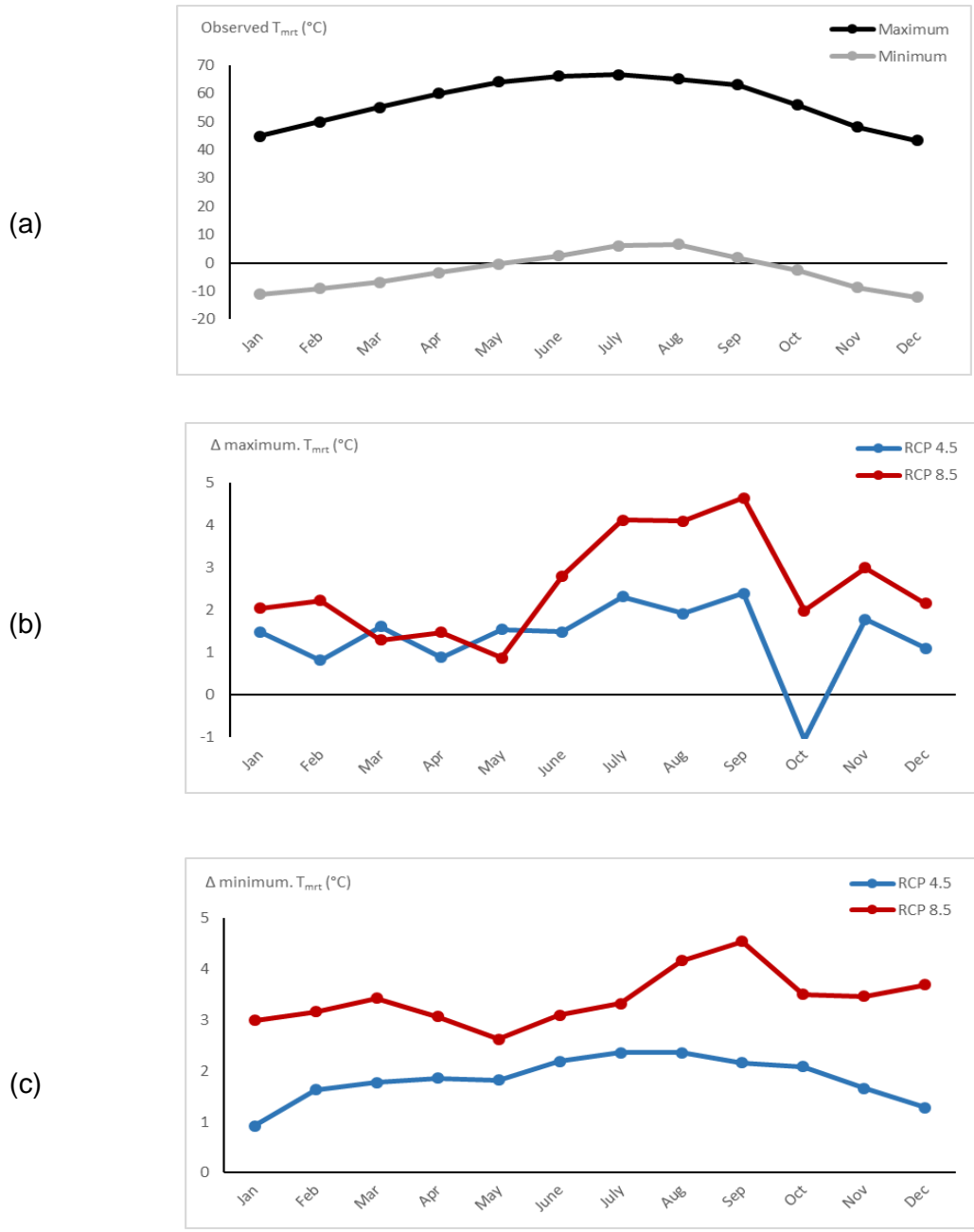


Figure 4-5: (a) Observed monthly-averaged daily maximum and minimum T_{mrt} across the annual cycle; (b) difference between observed and future RCP 4.5 and 8.5 scenarios in monthly-averaged daily maximum T_{mrt} across the annual cycle; (c) difference between observed and future RCP 4.5 and 8.5 scenarios in monthly-averaged daily minimum T_{mrt} across the annual cycle. Observation record is from 2008-2017 and climate scenarios are from 2070-2100.

These results are consistent with simulated future climate studies in cities with comparable climates to Vancouver. In a study conducted by Thorsson et al. (2017) that evaluated the effect of future climate on T_{mrt} , it was found that average summer daily minimum T_{mrt} over two time periods (2040-2069 and 2070-2098) increased, although with different magnitude, for all three European cities under investigation: Gothenburg (Sweden), Frankfurt (Germany) and Porto (Portugal). In a similar type of study, Zölch et al. (2016) found a 1°C increase in T_{mrt} in a high-density residential area of Munich, Germany under a downscaled future climate scenario of RCP 4.5 for the 2030-2060 time period.

The increased T_{mrt} result from projected climate scenarios, in our study, provides evidence that heat mitigation measures are needed to create thermally comfortable environments in Vancouver. In fact, the projected future changes in micrometeorological variables and the assessment of extreme radiant thermal exposure indicate that high T_{mrt} values and subsequent thermal exposure will further increase under RCP 4.5 and 8.5 scenarios over the 2070-2100 period.

Table 4-1: Average number of days per year, average number of consecutive days (two or more days) per year and average number of weeks (seven consecutive days) per year with $T_{mrt} \geq 65^\circ\text{C}$ for observation period, RCP 4.5 and 8.5 scenarios.

	Observation	RCP 4.5	RCP 8.5
Average number of days per year	8	23	40
Average number of consecutive days (two or more days) per year	6	19	33
Average number of weeks (seven consecutive days) per year	0.1	0.6	2.1
Average number of consecutive hours per year	16	48	94

4.4.3. The effect of street trees on T_{mrt}

Additional street trees were added to the simulations as a potential heat mitigation measure. The cooling effect of increasing the number of street trees up to their maximum feasible number was modelled and mapped (Figure 4-6). For the observation day (i.e. July 29,

2009), the results indicated reductions in T_{mrt} for all six LCZs, ranging from a 2.1°C decrease in LCZ 5 to a 4.2°C decrease in LCZ 8. This shows that trees in large low-rise open areas (i.e. LCZ 8) which are not already well-shaded by buildings or existing trees, reduce T_{mrt} more than they do for other LCZs in Vancouver. Under the maximum feasible street tree cover scenario, for RCP 4.5, T_{mrt} decreased by 1.3°C on average compared to the observation day with current street trees. However, an increase in T_{mrt} was evident for the RCP 8.5 scenario despite the added street tree cover. In fact, T_{mrt} increased in all LCZs under the RCP 8.5 climate scenario even with the applied heat mitigation measure (i.e. maximum feasible number of street trees). This is because the potential for increasing street tree cover relative to current status is very small in Vancouver’s LCZs (i.e. the maximum feasible number of street trees resulted in only 1.2% plan area increase in street tree cover). This has also been found in a study conducted in Manchester, UK, where increasing street tree cover to a maximum level (5% under current planting regulations for Manchester) was not sufficient to keep the temperatures at or below current levels under three climate scenarios (Hall et al. 2012).

Table 4-2: Spatial average of T_{mrt} values before and after adding maximum feasible street trees. Results are for the hottest period of day from 11:00 – 17:00 for the hottest day in the observation period, RCP 4.5 and 8.5. Δ indicates the difference in T_{mrt} relative to the observation day under current tree cover.

Location	Current status			Maximum feasible number of street trees		
	Observation	Δ RCP 4.5	Δ RCP 8.5	Δ Observation	Δ RCP 4.5	Δ RCP 8.5
	day			day		
LCZ 1	51.1	+2	+5.1	-3.3	-0.7	+2.6
LCZ 4	53.9	+1.7	+4.8	-3.5	-1.8	+1.4
LCZ 5	54.7	+1.7	+4.8	-2.1	-0.4	+2.8
LCZ 6	58.6	+1.7	+4.7	-4.1	-2.4	+0.8
LCZ 6A	59.6	+1.7	+4.7	-3.4	0	+3.1
LCZ 8	61.1	+1.7	+4.7	-4.2	-2.5	+0.7

In light of recent works suggesting that end-of-century urban air temperatures under the RCP 8.5 scenario cannot be offset by large street tree increases in combination with other heat mitigation measures at both neighborhood and regional scales (Krayenhoff et al. 2018;

Middel et al. 2015), a corresponding investigation of the potential for T_{mrt} reduction is of particular relevance. Thus, reducing T_{mrt} will have to be achieved through complementary heat mitigation measures, for instance through greening building facades (Jänicke et al. 2015), converting selected streets in high- T_{mrt} LCZs into greenways (Gill et al. 2007), and artificial solar shielding (Watkins et al. 2007).

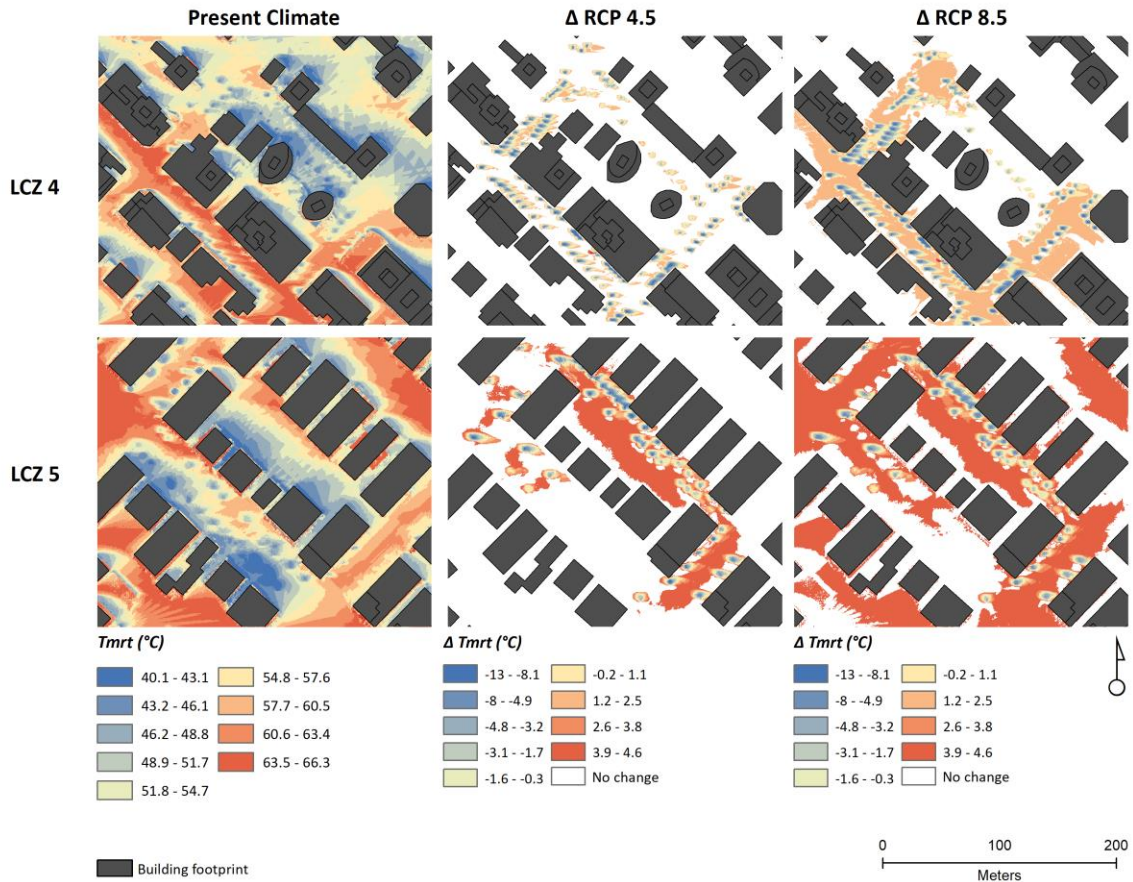


Figure 4-6: The spatial variation of T_{mrt} in present climate (left column) and the combined effect of climate change and increased street tree cover for RCP 4.5 and 8.5 scenarios (middle and right column). Δ RCP 4.5 and Δ RCP 8.5 present change in T_{mrt} values relative to the observation day after the inclusion of maximum feasible street tree in the simulation domain. The T_{mrt} values are averaged over the period from 11:00 – 17:00. For illustration purposes, the comparison is only shown for LCZ 4 and 5.

Aside from the benefit of street trees in reducing radiant heat load, adding excessive amounts of street trees may also have negative and unwanted effects. Due to the hampering effect of street trees on air ventilation at the microscale, roadside trees do not necessarily

reduce pollutant concentrations and can therefore worsen air quality in the immediate vicinity of streets (Vos et al. 2013). Trees also reduce radiative heat loss at night and slightly increase temperatures after sunset (Golden et al. 2007). Lastly, during the fall and winter season when unobstructed sunshine is desirable in mid-latitude cities such as Vancouver, excessive shade can be unwanted. In this respect, deciduous trees are preferred over evergreen trees as the former species allow 40 to 80% penetration of solar radiation in fall and winter (Heisler 1986; Konarska et al. 2014).

4.5. Conclusion

Present and future changes in micrometeorological variables (T_a , global radiation and T_{mrt}) were compared across the annual cycle, with major focus on the hottest time of day for the observation period and for an end-of-century hot day, for six different LCZs in Vancouver. In addition, the effect of increasing street tree cover on the spatial variation of T_{mrt} under two future climate scenarios, RCP 4.5 and 8.5, was modelled and mapped. Model simulations were conducted for two urban greening scenarios: a) the current street tree cover, and b) a simulated increase of street trees to the maximum feasible number in each LCZ.

In Vancouver, downscaled projections of RCP 4.5 and 8.5 scenarios showed an increased maximum and minimum T_a . Global radiation remains largely unchanged under the RCP 4.5 scenario, while it decreases slightly across the annual cycle under the RCP 8.5 scenario. The number of days with very high T_{mrt} , i.e. days with extreme radiant thermal exposure, is projected to increase three- and five-fold under RCP 4.5 and 8.5 respectively.

The cooling potential achieved by adding the maximum feasible number of street trees is effective in the reduction or maintenance of the current T_{mrt} under the RCP 4.5 scenario for all LCZs in Vancouver, however it is insufficient to decrease or maintain T_{mrt} under the RCP 8.5 scenario. Under the RCP 8.5 scenario, complimentary heat mitigation measures may be therefore required if summer outdoor thermal comfort is to be maintained or improved in Vancouver through the end of the century.

From an urban planning point of view, informed by the results of our analysis, this study recommends that an effective heat mitigation strategy: (a) prioritizes plans for LCZs in which extreme levels of T_{mrt} exist under present and future climates and in areas frequented by

pedestrians; (b) complements the mitigation effects of street trees by adding green walls and installing artificial solar shielding, especially in areas where extra tree planting is not practical due to limited planting space or high building density; and (c) considers tree placement with the goal of maximizing tree shade while limiting associated reductions to ventilation.

4.6. Acknowledgments

The author acknowledges support from the Pacific Institute for Climate Solutions (PICS) and The Mathematics of Information Technology and Complex Systems (MITACS) Globalink Research fellowship programs.

4.7. References

- Alexander, P.J., Fealy, R., and Mills, G.M., 2016. "Simulating the impact of urban development pathways on the local climate: a scenario-based analysis in the Greater Dublin region, Ireland." *Landscape and Urban Planning*. 152: 72–89.
- Ali-Toudert, F., and Mayer, H., 2007. "Effects of asymmetry, galleries, overhanging façades and vegetation on thermal comfort in urban street canyons." *Solar Energy*. 81 (6): 742–54.
- Aminipouri, M., Knudby, A., and Ho, H.C., 2016. "Using multiple disparate data sources to map heat vulnerability: Vancouver case study." *The Canadian Geographer*. 60 (3): 356–68.
- Aminipouri, M., Knudby, A., Krayenhoff, E.S., Zickfeld, K., and Middel, A., 2019. "Modelling the impact of increased street tree cover on mean radiant temperature across Vancouver's local climate zones." *Urban Forestry and Urban Greening*. 39: 9-17.
- Argüeso, D., Evans, J.P., Pitman, A.J., and Di Luca, A., 2015. "Effects of city expansion on heat stress under climate change conditions." *PLoS ONE*. 10 (2): 1–19.
- Arora, V. K., Scinocca, J.F., Boer, G.J., Christian, J.R., Denman, K.L., Flato, G.M., Kharin, V.V., Lee, W.G., and Merryfield, W.J., 2011. "Carbon emission limits required to satisfy future representative concentration pathways of greenhouse gases." *Geophysical Research Letters*. 38 (5).
- Baccini, M., Biggeri, A., Accetta, G., Kosatsky, T., Katsouyanni, K., and Analitis, A., 2008. "Heat effects on mortality in 15 European cities." *Epidemiology* 19: 711-719. doi: 10.1097/EDE.0b013e318176bfcd.
- Besancenot, J. P., 2002. "Heat waves and mortality in large urban areas." *Environnement, Risques & Sante* 1 (4): 229-240.
- Benestad, R E. 2011. "Empirical-statistical downscaling in climate modeling." *Eos, Transactions*

- American Geophysical Union*. 85 (42): 417–22.
- Benmarhnia, T., Sottile, M.F., Plante, C., Brand, A., Casati, B., Fournier, M., and Smargiassi, A., 2014. "Variability in temperature-related mortality projections under climate change." *Environmental Health Perspectives*. 122 (12): 1293–98.
- Chen, L., Yu, B., Yang, F., and Mayer, H., 2016. "Intra-urban differences of mean radiant temperature in different urban settings in Shanghai and implications for heat stress under heat waves: a GIS-based approach." *Energy and Buildings*. 130: 829–42.
- Chen, Y.C., Lin, T.P., and Matzarakis, A., 2014. "Comparison of mean radiant temperature from field experiment and modelling: a case study in Freiburg, Germany." *Theoretical and Applied Climatology*. 118 (3): 535–51.
- City of Vancouver. 2011. "Street tree guidelines." Vancouver.
- Gill, S.E., Handley, J.F., Ennos, A.R., and Pauleit, S., 2007. "Adapting cities for climate change: the role of the green infrastructure." *Built Environment*. 33 (1): 115–33.
- Golden, J.S., Carlson, J., Kaloush, K.E., and Phelan, P., 2007. "A comparative study of the thermal and radiative impacts of photovoltaic canopies on pavement surface temperatures." *Solar Energy*. 81 (7): 872–83.
- Goodman, P. G., Dockery, D. W., and Clancy, L., 2004. "Cause- specific mortality and the extended effects of particulate pollution and temperature exposure." *Environmental Health Perspectives* 112 (2): 179-185.
- Hall, J.M., Handley, J.F., and Ennos, A.R., 2012. "The potential of tree planting to climate-proof high density residential areas in Manchester, UK." *Landscape and Urban Planning*. 104 (3–4): 410–17.
- Heisler, G. M., 1986. "Energy savings with trees." *Journal of Arboriculture*. 12 (5): 113–25.
- Ho, H.C., Knudby, A., Xu, Y., Hodul, M., and Aminipouri, M., 2015. "A comparison of urban heat islands mapped using skin temperature, air temperature, and apparent temperature (Humidex), for the Greater Vancouver area." *The Science of the Total Environment*. 544: 929–38.
- Ho, H.C., Knudby, A., Chi, G., Aminipouri, M., Lai, D.Y.F., 2018. "Spatiotemporal analysis of regional socio-economic vulnerability change associated with heat risks in Canada." *Applied Geography*. 95: 61-70.
- Holst, J., and Mayer, H., 2010. "Urban human-biometeorology: investigations in Freiburg (Germany) on human thermal comfort." *Urban Climate News*. 38. 5-10.
- Höppe, P., 1999. "The physiological equivalent temperature - a universal index for the biometeorological assessment of the thermal environment." *International Journal of Biometeorology*. 43 (2): 71–75.

- Jänicke, B., Meier, F., Hoelscher, M.T., and Scherer, D., 2015. "Evaluating the effects of facade greening on human bioclimate in a complex urban environment." *Advances in Meteorology*, 1–15.
- Jendritzky, G., de Dear, R., and Havenith, G., 2012. "UTCI-why another thermal index?" *International Journal of Biometeorology*. 56 (3): 421–28.
- Koffi, B., and Koffi, E., 2008. "Heat waves across Europe by the end of the 21st century: multiregional climate simulations ." *Climate Research*. 36 (2): 153–68.
- Konarska, J., Lindberg, F., Larsson, A., Thorsson, S., and Holmer, B., 2014. "Transmissivity of solar radiation through crowns of single urban trees - application for outdoor thermal comfort modelling." *Theoretical and Applied Climatology*. 117 (3): 363–76.
- Kong, L., Lau, K.K.L., Yuan, C., Chen, Y., Xu, Y., Ren, C., and Ng, E., 2017. "Regulation of outdoor thermal comfort by trees in Hong Kong." *Sustainable Cities and Society*. 31: 12–25.
- Krayenhoff, E. S., Moustou, M., Broadbent, A.M., Gupta, V., and Georgescu, M., 2018. "Diurnal interaction between urban expansion, climate change and adaptation in US cities." *Nature Climate Change*. 8 (12): 1097–1103.
- Laaidi, K., Zeghnoun, A., Dousset, B., Bretin, P., Vandentorren, S., Giraudet, E., and Beaudeau, P., 2012. "The impact of heat islands on mortality in Paris during the August 2003 heat wave." *Environmental Health Perspectives* 120 (2): 254-259.
- Lau, K.K.L., Lindberg, F., Rayner, D., and Thorsson, S., 2014. "The effect of urban geometry on mean radiant temperature under future climate change: a study of three European cities." *International Journal of Biometeorology*. 59 (7): 799–814.
- Lau, K.K.L., Ren, C., Ho, J., and Ng, E., 2016. "Numerical modelling of mean radiant temperature in high-density sub-tropical urban environment." *Energy and Buildings*. 114: 80–86.
- Lee, H., Holst, J., and Mayer., 2013. "Modification of human-biometeorologically significant radiation flux densities by shading as local method to mitigate heat stress in summer within urban street canyons." *Advances in Meteorology* 2013. 13.
- Lee, H., Mayer, H., and Chen, L., 2016. "Contribution of trees and grasslands to the mitigation of human heat stress in a residential district of Freiburg, Southwest Germany." *Landscape and Urban Planning*. 148: 37–50.
- Lindberg, F., Holmer, B., and Thorsson, S., 2008. "SOLWEIG 1.0 - modelling spatial variations of 3D radiant fluxes and mean radiant temperature in complex urban settings." *International Journal of Biometeorology*. 52 (7): 697–713.
- Lindberg, F., and Grimmond, C.S.B., 2011a. "Nature of vegetation and building morphology characteristics across a city: influence on shadow patterns and mean radiant temperatures in London." *Urban Ecosystems*. 14 (4): 617–34.
- Lindberg, F., and Grimmond, C.S.B., 2011b. "The influence of vegetation and building

- morphology on shadow patterns and mean radiant temperatures in urban areas: model development and evaluation." *Theoretical and Applied Climatology*. 105 (3): 311–23.
- Lindberg, F., Holmer, B., Thorsson, S., and Rayner, D., 2014. "Characteristics of the mean radiant temperature in high latitude cities - implications for sensitive climate planning applications." *International Journal of Biometeorology*. 58 (5): 613–27.
- Lindberg, F., Thorsson, S., Rayner, D., and Lau, K.K.L., 2016. "The impact of urban planning strategies on heat stress in a climate-change perspective." *Sustainable Cities and Society*. 25: 1–12.
- Lobaccaro, G., and Acero, J.A., 2015. "Comparative analysis of green actions to improve outdoor thermal comfort inside typical urban street canyons." *Urban Climate*. 14: 251–67.
- Mayer, H., Holst, J., Dostal, P., Imbery, F., and Schindler, D., 2008. "Human thermal comfort in summer within an urban street canyon in central Europe." *Meteorologische Zeitschrift*. 17 (3): 241–50.
- Metro Vancouver. 2016. "Climate projections for Metro Vancouver."
- Middel, A., Chhetri, N., Quay, R., 2015. "Urban forestry and cool roofs: Assessment of heat mitigation strategies in Phoenix residential neighborhoods." *Urban Forestry & Urban Greening*. 14(1): 178-186.
- Middel, A., Selover, N., Hagen, B., and Chhetri, N., 2016. "Impact of shade on outdoor thermal comfort - a seasonal field study in Tempe, Arizona." *International Journal of Biometeorology*, 1–13.
- Moss, R.H., Edmonds, J.A., Hibbard, K.A., Manning, M.R., Rose, S.K., van Vuuren, D.P., Carter, T.R., 2010. "The next generation of scenarios for climate change research and assessment." *Nature*. 463: 747.
- Ng, W.Y., Chau, C.K., Powell, G., and Leung, T.M., 2015. "Preferences for street configuration and street tree planting in urban Hong Kong." *Urban Forestry & Urban Greening*. 14 (1): 30–38.
- Oke, T.R., and Cleugh, H.A., 1987. "Urban heat storage derived as energy balance residuals." *Boundary-Layer Meteorology*. 39 (3): 233–45.
- Oliveira, S., Andrade, H., and Vaz, T., 2011. "The cooling effect of green spaces as a contribution to the mitigation of urban heat: a case study in Lisbon." *Building and Environment*. 46 (11): 2186–94.
- Onomura, S., Grimmond, C.S.B., Lindberg, F., Holmer, B., and Thorsson, S., 2015. "Meteorological forcing data for urban outdoor thermal comfort models from a coupled convective boundary layer and surface energy balance scheme." *Urban Climate*. 11: 1–23.
- Open Data Catalogue, 2019. Open Data Catalogue City of Vancouver. Accessed online at.on June

- 24, 2019. <https://data.vancouver.ca/datacatalogue/index.htm>
- Pantavou, K., Lykoudis, S., Nikolopoulou, M., and Tsiros, L.X., 2018. "Thermal sensation and climate: a comparison of UTCI and PET thresholds in different climates." *International Journal of Biometeorology*. 62 (9): 1695–1708.
- Park, J.H., Kim, J., Yoon, D.K., and Cho, G.H., 2016. "The influence of Korea's green parking project on the thermal environment of a residential street." *Habitat International*. 56: 181–90.
- Park, S., Tuller, S.E., and Jo, M., 2014. "Application of universal thermal climate index (UTCI) for microclimatic analysis in urban thermal environments." *Landscape and Urban Planning*. 125: 146–55.
- Rayner, D., Lindberg, F., Thorsson, S., and Holmer, B., 2015. "A statistical downscaling algorithm for thermal comfort applications." *Theoretical and Applied Climatology*. 122 (3): 729–42.
- Reindl, D.T., Beckman, W.A., and Duffie, J.A., 1990. "Diffuse fraction correlations." *Solar Energy*. 45 (1): 1–7.
- Riahi, K., Steven, R., Runci, P., Stouffer, R., van Vuuren, D., Weyant, J., Wilbanks, T., van Ypersele, J.P., and Zurek, M., 2008. "Towards new scenarios for analysis of emissions, climate change impacts and response strategies." Geneva, Switzerland.
- Rivington, M., Miller, D., Matthews K.B., Russell, G., Bellocchi, G., and Buchan, K., 2008. "Downscaling regional climate model estimates of daily precipitation, temperature and solar radiation data ." *Climate Research*. 35 (3): 181–202.
- Runnalls, K.E., and Oke, T.R., 2000. "Dynamics and controls of the near-surface heat island of Vancouver, British Columbia." *Physical Geography* 21 (4): 283–304.
- Scinocca, J.F., Kharin, V.V., Jiao, Y., Qian, M.W., Lazare, M., Solheim, L., Flato, G.M., Biner, S., Desgagne, M., and Dugas, B., 2016. "Coordinated global and regional climate modeling." *Journal of Climate*. 29 (1): 17–35.
- Shashua-Bar, L., Pearlmutter, D., and Erell, E., 2011. "The influence of trees and grass on outdoor thermal comfort in a hot-arid environment." *International Journal of Climatology*. 31 (10): 1498–1506.
- Stewart, I.D., and Oke, T.R., 2012. "Local climate zones for urban temperature studies." *Bulletin of the American Meteorological Society*. 93 (12): 1879–1900.
- Stewart, I.D., 2011. "Redefining the urban heat island." Ph.D Thesis, University of British Columbia, Vancouver, Canada.
- Steyn, D.G., and Oke, T.R., 1980. "Effects of a small scrub fire on the surface radiation budget." *Weather*. 35 (7): 212–15.
- Thom, J.K., Coutts, A.M., Broadbent, A.M., and Tapper, N.J., 2016. "The influence of increasing

- tree cover on mean radiant temperature across a mixed development suburb in Adelaide, Australia." *Urban Forestry & Urban Greening*. 20: 233–42.
- Thorsson, S., Lindberg, F., Eliasson, I., and Holmer, B., 2007. "Different methods for estimating the mean radiant temperature in an outdoor urban setting." *International Journal of Climatology*. 27 (14): 1983–93.
- Thorsson, S., Rayner, D., Lindberg, F., Monteiro, A., Katschner, L., Lau, K.K.L., Campe, S., 2017. "Present and projected future mean radiant temperature for three European cities." *International Journal of Biometeorology*. 61 (9): 1531–43.
- Thorsson, S., Rocklov, J., Konarska, J., Lindberg, F., Holmer, B., Dousset, B., and Rayner, D., 2014. "Mean radiant temperature: a predictor of heat related mortality." *Urban Climate*. 10: 332–45.
- Voogt, J. A., and Oke, T.R., 1997. "Complete urban surface temperatures." *Journal of Applied Meteorology*. 36.
- Vos, P.E.J., Maiheu, B., Vankerkom, J., and Janssen, S., 2013. "Improving local air quality in cities: to tree or not to tree?" *Environmental Pollution*. 183: 113–22.
- Wang, X., Huang, G., Liu, J., Li, Z., and Zhao, S., 2015. "Ensemble projections of regional climatic changes over Ontario, Canada." *Journal of Climate*. 28 (18): 7327–46.
- Watkins, R., Palmer, J., and Kolokotroni, M., 2007. "Increased temperature and intensification of the urban heat island: implications for human comfort and urban design." *Built Environment*. 33 (1): 85–96.
- Yang, S.R., and Lin, T.P., 2016. "An integrated outdoor spaces design procedure to relieve heat stress in hot and humid regions." *Building and Environment*. 99: 149–60.
- Zölch, T., Maderspacher, J., Wamsler, C., and Pauleit, S., 2016. "Using green infrastructure for urban climate-proofing: an evaluation of heat mitigation measures at the micro-scale." *Urban Forestry & Urban Greening*. 20: 305–16.

Chapter 5. Conclusions

In the following sections, the overall contributions of this thesis and a summary and discussion of the key contributions of each paper is presented. General conclusions of this work are also outlined.

5.1. Overall contributions

This thesis implements geographic qualitative, quantitative and modelling techniques to: a) explore how heat vulnerability varies among different neighborhoods in Vancouver; and b) investigate heat mitigation through urban tree planting across Vancouver's local climate zones (LCZs), focusing on the impact of added street trees on human thermal exposure under current and projected future climates.

This thesis is unique in its approach toward quantifying and mapping human thermal exposure in different neighbourhoods, categorized into LCZs. This is done for the first time in a mid-latitude coastal city. Furthermore, the characterization of baseline radiant heat exposure across Vancouver's LCZs during summertime extreme heat days, prior to and after heat mitigation implementations under current and future climates, is unique to this study. The results from this thesis can inform decision-makers and provide tools to facilitate the integration of microclimate knowledge into urban design and planning practices for Vancouver.

The following are the main contributions drawn from each chapter:

- Chapter 2: considering existing socio-economic, environmental and infrastructural data, populations vulnerable to extreme heat were mapped at dissemination area scale in Vancouver. Using a spatial overlay analysis, neighborhoods that are particularly vulnerable to heat in terms of the compound effect of low socioeconomic status, high heat exposure and poor accessibility to cooling and health infrastructures were identified. The top three vulnerable neighborhoods, located in the Sunset neighbourhood of southeast Vancouver, were characterized by low vegetation cover, relatively hot surface and near-surface air temperatures, low socioeconomic status, far

from cooling and health infrastructure, and have an environment that elevates heat exposure. Some of these heat-vulnerable neighborhoods which are classified as LCZ 6 were used as case studies in which the impact of heat mitigation measures on heat exposure is further examined in Chapter 3 and 4. The applied methodology in this chapter was largely qualitative and exploratory, coupled with spatial overlay mapping techniques. One of the strengths of this work is the ability to produce readily available information about heat vulnerability status. The approach taken in this chapter can be considered a first step toward the development of tools that can help health authorities, city officials, and policymakers better understand who is at risk during extreme heat events, where these people reside, and what factors drive their local risk. Appreciation of this multi-faceted context can facilitate both short-term emergency management efforts and longer-term urban planning interventions to reduce health effects of extreme heat events with greater effectiveness. While only Vancouver neighborhoods were investigated in this chapter, the proposed methodology is easily transferable to other cities in Canada and worldwide.

- Chapter 3: this chapter contributes to better understanding about how the built environment influences the effectiveness of heat mitigation measures across Vancouver's LCZs. Specifically, this chapter contributes to quantifying the impact of added street trees on radiant heat exposure. This was achieved by evaluating the spatiotemporal variation of radiant heat exposure, and its daytime reductions resulting from increased street tree cover within street sections of representative LCZs in Vancouver. LCZ 1 (compact high-rise) and LCZ 8 (large low-rise) were identified as the most and least thermally comfortable LCZs in Vancouver, respectively. Increasing street tree cover showed significant impact on reducing heat exposure by lowering T_{mrt} by minimum 3.3°C in LCZ 1 (compact high-rise) to maximum 7.1°C in LCZ 6 (open low-rise). The urban tree-planting scenario applied in this chapter (i.e. 1% increase in aerial street tree coverage) was adopted from Vancouver's urban forestry strategy that aims to grow its aerial urban canopy cover by 1% by the year 2020.
- Chapter 4: this chapter expands on the findings from Chapter 3 and provides a methodology that quantifies how radiant heat exposure may be affected under future climate change projections. This chapter also illustrates how days with extreme radiant

heat exposure will become more frequent under future climate scenarios (RCP 4.5 and 8.5). The results show that the net effect of urban tree planting on reducing radiant heat exposure varies between RCP 4.5 and 8.5 scenarios. Under the maximum feasible street tree cover scenario, spatial average net change of T_{mrt} is a 1.3°C reduction under RCP 4.5 compared to the same time of day for the hottest day in the contemporary period, whereas spatial average net change of T_{mrt} was a 1.9°C increase under RCP 8.5. This chapter concludes by presenting a set of complementary heat mitigation guidelines applicable to urban planning.

5.2. Discussion

The qualitative data collection approach and spatial overlay analysis presented in Chapter 2 were useful in identifying and mapping heat-vulnerable neighbourhoods. However, the main limitation of this methodology is that the presented results were not validated against individual-level socio-economic data, nor against data on health or other impacts of recent extreme heat events. In this case, validation was beyond reach as it was very difficult to obtain comprehensive social survey data across Vancouver at neighborhood scales. Nonetheless, evaluating the results against individual-level socio-economic and health data would have enhanced the results of this study as it could exhibit that in reality the vulnerability characteristics exist in identified neighborhood.

Similar to any modelling study, the simulation results in Chapter 3 and 4 were dependent on the accuracy of the inputs, namely, digital surface model of buildings and trees, sky view factor, and forcing micrometeorological variables. Based on the model evaluation results presented in Chapter 3, it was concluded that the input data were of high quality. Regarding the spatial variability of T_{mrt} , this thesis showed that the addition of street trees and the shadow they provide is a very effective measure for reducing daytime T_{mrt} in urban neighborhoods during hot summer days. Although the reduction of T_{mrt} is dependent on the size and shape of individual trees, the placement (e.g. closer to sun-exposed walls), clustering and different tree species affect T_{mrt} reductions (Konarska et al. 2014; Lindberg et al. 2016). However, the effect of different tree species, tree sizes and tree clustering were not explored in this thesis.

Due to the structure of the SOLWEIG model, which relies on incoming solar radiation, this thesis only focused on daytime variations of T_{mrt} . In other words, SOLWEIG is unable to assess the effect of added street trees on nocturnal radiant heat exposure. Nighttime heat exposure (i.e. T_{mrt}) is of great importance, since it is attributed to extreme heat stress and heat-related mortality (Thorsson et al. 2014). Raised nighttime minimum mean radiant temperature, which in part results from the reduced escape of longwave radiation blocked under tree canopy, can further increase heat stress and potentially lead to heat-related mortality (Lindberg et al. 2016; Thorsson et al. 2014). It has been found that heat-related mortality is strongly associated with exposure to a high nighttime temperature over several days, especially among elderly individuals (Luber and McGeehin 2008; Laaidi et al. 2012). For example, an estimated 0.8% increase in heat-related deaths was found to be correlated with 1°C increase in nighttime air temperature in Dublin, Ireland (Goodman et al. 2004). In a case study in Stockholm (1990-2002), Thorsson et al. (2014) found that for ages 45-79 heat related mortality is more attributed to nighttime rather than daytime heat stress resulted from increased radiant heat exposure.

This thesis focused on only one heat exposure metric, T_{mrt} , and hence is an incomprehensive representation of thermal comfort (Lindberg et al. 2016). Two other important factors for radiant heat exposure and outdoor thermal comfort that are not considered by T_{mrt} , are air flow and clothing insulation. Air flow affects thermal comfort by contributing to convective cooling of the human body and reducing heat stress (Saneinejad et al. 2014; Toparlar et al. 2015). Clothing insulation affects thermal comfort through heat transfer and evaporation of moisture from the skin (Jendritzky et al. 2012). Efforts are being made to include pedestrian wind field and clothing insulation in the future versions of SOLWEIG (Linberg et al. 2016).

In Chapter 4, only one regional climate model (CanRCM4) were incorporated in the simulations. Generally, the performance (i.e. analysis of errors and biases) of CanRCM4 in reproducing the spatial pattern, annual cycle and distribution of extreme temperatures falls within the range of other North American RCMs (Scinocca et al. 2015). However, when compared to the fifth-generation Canadian regional climate model (CRCM5) for example, CanRCm4 shows larger discrepancy (i.e. regional root mean square error) in the simulation of the hottest day (+0.8°C) and the coolest night (+2.7°C) over the period 1989–2009 (Whan and Zwiers 2015). Therefore, it would be beneficial if outputs from a greater range of RCMs are investigated to identify biases in temperature extremes.

5.3. General conclusion and future outlook

In the context of both global warming and rapidly growing urbanization worldwide, urban dwellers are likely to become more exposed to extreme radiant heat.

This thesis assessed the variability of heat vulnerability and radiant heat exposure across neighborhoods in Vancouver. Specifically, the determinants of heat vulnerability in Vancouver were explored (Chapter 2), and increased street tree cover was tested as a heat mitigation strategy to lower radiant heat exposure in different neighborhoods under current and future climates (Chapter 3 and 4). This thesis has evaluated the effectiveness of urban tree planting in reducing radiant heat exposure. For example, added street trees can largely mitigate the increased radiant heat exposure expected by 2070-2100 under RCP 4.5. However, the mitigating effect of added street trees on radiant heat exposure is not sufficient to similarly compensate for the impacts of global warming under the RCP 8.5 scenario. This type of information can inform city decision-makers and urban planners on ways to prioritize heat mitigation and adaptation interventions.

The insights and limitations of this thesis provide a potential pathway for future research. Simulation of radiant heat exposure with different tree clustering scenarios, combined with other heat mitigation and emission reduction measures, and under downscaled projections from various RCMs would increase our understanding of the relative effectiveness of urban tree planting practices on intra-urban radiant heat exposure variations and its dependence on local micrometeorological conditions. Considering the implications of urban tree planting on thermal exposure, it would be of further research interest to compare the findings of this thesis with people's perception of the effect of urban street tree planting on neighborhood microclimate as well as human thermal comfort.

5.4. References

Goodman, P. G., Dockery, D. W., and Clancy, L., 2004. "Cause-specific mortality and the extended effects of particulate pollution and temperature exposure." *Environmental Health Perspectives* 112 (2): 179-185.

- Jendritzky, G., de Gear, R., Havenith, G., 2012. "UTCI – Why another thermal index?" *International Journal of Biometeorology*. 56 (3): 421-428.
- Konarska, J., Lindberg, F., Larsson, A., Thorsson, S., Holmer, B., 2014. "Transmissivity of solar radiation through crowns of single urban trees: application for outdoor thermal comfort modelling." *Theoretical and Applied Climatology* 117: 363-376.
- Laaidi, K., Zeghnoun, A., Dousset, B., Bretin, P., Vandentorren, S., Giraudet, E., and Beaudeau, P., 2012. "The impact of heat islands on mortality in Paris during the August 2003 heat wave." *Environmental Health Perspectives* 120 (2): 254-259.
- Lindberg, F., Thorsson, S., Rayner, D., Lau, K., 2016. "The impact of urban planning strategies on heat stress in a climate-change perspective." *Sustainable Cities and Society* 25: 1-12.
- Luber, G., McGeehin, M., 2008. "Climate change and extreme heat events." *American Journal of Preventive Medicine* 35 (5): 429-435.
- Saneinejad, S., Moonen, P., Carmeliet, J., 2014. "Coupled CFD, radiation and porous media model for evaluating the micro-climate in an urban environment." *Journal of Wind Engineering and Industrial Aerodynamics*. 128: 1-11.
- Scinocca, J.F., Kharin, V.V., Jiao, Y., Qian, M.W., Lazare, M., Solheim, L., Flato, G.M., 2015. "Coordinated global and regional climate modeling." *Journal of Climate*. 29, 17-35.
- Thorsson, S., Rocklov, J., Konarska, J., Lindberg, F., Holmer, B., Dousset, B., Rayner, D., 2014. "Mean radiant temperature – a predictor of heat related mortality." *Urban Climate*. 10 (2): 332-345.
- Toparlar, Y., Blocken, B., Vos, P., van Heijst, G.J.F., Janssen, W.D., van Hooff, T., 2015. "CFD simulation and validation of urban microclimate: a case study for Bergpolder Zuid, Rotterdam." *Building and Environment*. 83: 79-90.
- Whan, K., Zwiers, F., 2015. "Evaluation of extreme rainfall and temperature over North America in CanRCM4 and CRCM5." *Climate Dynamics*. 46 (11-12): 3821-3843.